© 2020. Published by The Company of Biologists Ltd | Development (2020) 147, dev185116. doi:10.1242/dev.185116

RESEARCH REPORT

Zebrafish Hif3α modulates erythropoiesis via regulation of *gata1* to facilitate hypoxia tolerance

Xiaolian Cai[1,4], Ziwen Zhou[1,4], Junji Zhu[1,4], Qian Liao[1,4], Dawei Zhang[1], Xing Liu[1,2,5], Jing Wang[1,2,5], Gang Ouyang[1,2,5] and Wuhan Xiao[1,2,3,4,5,*]

ABSTRACT

The hypoxia-inducible factors 1α and 2α (HIF1α and HIF2α) are master regulators of the cellular response to O_2. In addition to HIF1α and HIF2α, HIF3α is another identified member of the HIFα family. Even though the question of whether some HIF3α isoforms have transcriptional activity or repressive activity is still under debate, it is evident that the full length of HIF3α acts as a transcription factor. However, its function in hypoxia signaling is largely unknown. Here, we show that loss of *hif3a* in zebrafish reduced hypoxia tolerance. Further assays indicated that erythrocyte number was decreased because red blood cell maturation was impeded by *hif3a* disruption. We found that *gata1* expression was downregulated in *hif3a* null zebrafish, as were several hematopoietic marker genes, including *alas2*, *band3*, *hbae1*, *hbae3* and *hbbe1*. Hif3α recognized the hypoxia response element located in the promoter of *gata1* and directly bound to the promoter to transactivate *gata1* expression. Our results suggested that *hif3a* facilities hypoxia tolerance by modulating erythropoiesis via *gata1* regulation.

KEY WORDS: *hif3a*, *gata1*, Zebrafish, Hypoxia, Erythropoiesis

INTRODUCTION

O_2 is indispensable for the survival of aerobic organisms (Aragonés et al., 2009; Majmundar et al., 2010; Semenza, 2014). Organisms have evolved sophisticated cellular sensors that respond to O_2 gradients (Bigham and Lee, 2014; Prabhakar and Semenza, 2015, 2016). Hypoxia is condition characterized by low ambient O_2, triggering acute and chronic organismal responses and inducing the expression of numerous genes (Semenza, 2014; Aragonés et al., 2009; Greer et al., 2012; Prabhakar and Semenza, 2012; Semenza, 2012; Shen and Kaelin, 2013). Hif1α (Hif1ab) and Hif2α (Epas1b) are regulators of the cellular response to O_2 (Majmundar et al., 2010; Semenza, 2012, 2014). Under normoxia, Phd1, Phd2, and Phd3 (Egln3) use O_2 and 2-oxoglutarate as substrates for the hydroxylation of Hif1α and Hif2α. Hydroxylated Hif1α and Hif2α are bound by VHL protein. VHL recruits a ubiquitin ligase complex that targets Hif1α and Hif2α for proteasomal degradation. Hypoxia inhibits Phd enzymatic activity, preventing the Phds from hydroxylating Hif1α and Hif2α. This results in Hifα protein stabilization and the induction of transcriptional activity (Bishop and Ratcliffe, 2015; Semenza, 2014).

Hif3α (Hif1al) is another Hifα protein (Augstein et al., 2011; Duan, 2016; Ravenna et al., 2016). Different from Hif1α and Hif2α, Hif3α comprises a transactivation domain (TAD), a leucine zipper domain (LZIP), and an LXXLL motif (Gu et al., 1998; Zhang et al., 2012). Therefore, Hif3α may be functionally distinguishable from Hif1α and Hif2α. Mammalian *HIF3a* genes use different promoters, different transcription initiation sites and alternative splicing to transcribe a large number of mRNA variants (Duan, 2016). Some of the short HIF3α isoforms lack TADs (Hara et al., 2001), and others have weak or absent transcriptional activity (Gu et al., 1998; Pasanen et al., 2010). Moreover, the overexpression of some HIF3α isoforms suppresses HIF1α- and/or HIF2α-induced reporter activity in cells (Maynard et al., 2003; Makino et al., 2001, 2007; Yamashita et al., 2008). Thus, it has been widely accepted that HIF3α acts as a negative regulator of HIF1α and HIF2α, even though, to date, only partial variants of mammalian HIF3α transcripts have been investigated, mostly via overexpression in cell culture systems with artificial reporter constructs (Duan, 2016; Ravenna et al., 2016). However, multiple lines of evidence support that the full length of HIF3α acts as a transcription factor (Duan, 2016; Heikkilä et al., 2011; Zhang et al., 2014; Zhou et al., 2018).

Interestingly, in zebrafish, only two isoforms of Hif3α (Hif3α/Hif3α1 and Hif3α2) have been identified (Zhang et al., 2016, 2012, 2014; Makino et al., 2001). Zebrafish Hif3α is a hypoxia-induced transcription factor that activates gene expression distinct from HIF1α (Zhang et al., 2014), whereas Hif3α2 is an oxygen-insensitive nuclear protein that inhibits canonical Wnt signaling by binding to β-catenin and destabilizing the nuclear β-catenin complex (Zhang et al., 2016).

To date, the roles of Hif3α in hypoxia signaling, and the mechanisms underlying these roles, are almost entirely unclear. Here, we knocked out *hif3a* in zebrafish and found that the resulting mutants exhibited increased sensitivity to hypoxia and reduced erythropoiesis. Our mechanistic studies indicated that Hif3α acted as a transcription factor and directly regulated *gata1* expression.

RESULTS AND DISCUSSION

Loss of *hif3a* in zebrafish reduced hypoxia tolerance

Zebrafish carry two isoforms of *hif3a*: *hif3a/hif3a1* (herein referred to as *hif3a*) and *hif3a2* (Fig. S1A,B; Zhang et al., 2016, 2012, 2014). We designed two gRNAs to disrupt the expression of this gene (Fig. S1A). Two mutants in the *hif3a* gene – *hif3a*$^{ihb20180620/ihb20180620}$ (http://zfin.org/ZDB-ALT-180620-1), herein designated M1, and *hif3a*$^{ihb20180621/ihb20180621}$ (http://zfin.org/ZDB-ALT-180620-2), herein designated M2 – were screened (Fig. S1A-C). The mutant *hif3a* encoded two truncated peptides (Fig. S1B). *hif3a* mRNA

[1]State Key Laboratory of Freshwater Ecology and Biotechnology, Institute of Hydrobiology, Chinese Academy of Sciences, Wuhan, 430072, China. [2]The Key Laboratory of Aquaculture Disease Control, Ministry of Agriculture, Institute of Hydrobiology, Chinese Academy of Sciences, Wuhan, 430072, China. [3]The Key Laboratory of Aquatic Biodiversity and Conservation, Institute of Hydrobiology, Chinese Academy of Sciences, Wuhan, 430072, China. [4]University of Chinese Academy of Sciences, Beijing, 100049, China. [5]The Innovation of Seed Design, Chinese Academy of Sciences, Wuhan, 430072, China.

*Author for correspondence (w-xiao@ihb.ac.cn)

W.X., 0000-0002-2978-0616

Handling Editor: Gordon Keller
Received 8 October 2019; Accepted 24 September 2020

Development (2020) 147, dev185116. doi:10.1242/dev.185116

expression was largely downregulated in the two mutants compared with the wild type (WT; Fig. S1D). An anti-Hif3α antibody had been developed and confirmed to recognize zebrafish Hif3α protein specifically (Zhang et al., 2012). Using western blot analysis, Hif3α protein could not be detected in the mutant (Fig. S1E). Overall, *hif3a*$^{-/-}$ zebrafish were identical to their WT siblings (*hif3a*$^{+/+}$) under normal conditions. Of note, the predicted truncated peptide of M1 contains the basic helix-loop-helix (bHLH) domain and that of M2 contains bHLH-PAS-PAC-ODD domains. The bHLH domain is important for DNA binding and dimerization with Hif1β. The PAS-A/B and PAC domains are also involved in Hif1β for dimerization (Semenza, 2014). To determine whether M1 and/or M2 mutant proteins may act in a dominant-negative manner, we examined overexpression of the predicted truncated peptides of M1 and M2 on a hypoxia response element (HRE)-luciferase reporter activity. As shown in Fig. S2A-C, overexpression of the predicted truncated peptides of M1 and M2 had no effect on the transcriptional activity of *hif1ab*, *hif2ab* and *hif3a* in epithelioma papulosum cyprini (EPC) cells. In the following experiments, we primarily used mutant M1 (*hif3a*$^{ihb20180620/ihb20180620}$) for phenotype analysis, and confirmed the observed M1 phenotypes in M2 (*hif3a*$^{ihb20180621/ihb20180621}$) to exclude off-targeting effects.

Given that Hif3α has been identified as an oxygen-dependent factor (Zhang et al., 2014), we aimed to determine whether disruption of *hif3a* impacted zebrafish hypoxia tolerance (Cai et al., 2018). In this study, after exposing *hif3a*$^{+/+}$ and *hif3a*$^{-/-}$ larvae to 2% O_2 simultaneously for 12 h, more *hif3a*$^{-/-}$ larvae were dead than *hif3a*$^{+/+}$ larvae (Fig. 1A,B). Under normoxia (21% O_2), no significant differences were detected between *hif3a*$^{+/+}$ and *hif3a*$^{-/-}$ larvae (Fig. 1A,D).

Subsequently, we measured the hypoxia tolerance of adult zebrafish [3 months post fertilization (mpf)]. When *hif3a*$^{+/+}$ and *hif3a*$^{-/-}$ adults with similar body weights (0.32±0.02 g; mean±s.d.) were subjected to hypoxia (5% O_2, adjusted before experimentation) simultaneously for 30 min, there were no obvious differences in behavior (Movie 1). However, as the duration of hypoxia increased, two *hif3a*$^{-/-}$ zebrafish appeared dead or near dead, whereas three *hif3a*$^{+/+}$zebrafish remained active (Movie 2).

We then tested *hif3a*$^{+/+}$ and *hif3a*$^{-/-}$ adults (6 mpf), with similar body weights (0.65±0.02 g), which were subjected to hypoxia (5% O_2, adjusted before experimentation). After 30 min, no significant difference in behaviors was observed between the *hif3a*$^{+/+}$ and *hif3a*$^{-/-}$ (Fig. 1C). However, *hif3a*$^{-/-}$ began to die after 46 min of hypoxia. After 50 min of hypoxia, all *hif3a*$^{-/-}$ zebrafish were dead, and all *hif3a*$^{+/+}$ zebrafish were still alive (Fig. 1C). Therefore, *hif3a*$^{-/-}$ zebrafish were more sensitive to hypoxia than *hif3a*$^{+/+}$ zebrafish.

We investigated whether the difference in hypoxia tolerance exhibited between *hif3a*$^{+/+}$ and *hif3a*$^{-/-}$ zebrafish was due to *hif3a*$^{-/-}$ zebrafish having higher oxygen consumption. Unexpectedly, in fact, the oxygen consumption rate of the *hif3a*$^{+/+}$ was even higher than that of the *hif3a*$^{-/-}$ (Fig. 1E), indicating that the oxygen consumption is not the cause. In order to validate the fact that the dissolved O_2 in water of the flasks is actually correlated with the O_2 concentration previously adjusted in the hypoxia workstation, we measured the dissolved O_2 in water with an LDO101 probe at different time points when the flasks were put into the hypoxia workstation set at 5% O_2 and 2% O_2 respectively (Fig. S2D,E). As expected, the dissolved O_2 in the water in the 2% O_2 workstation decreased faster than that in the 5% O_2 workstation, suggesting a precise correlation (Fig. S2D,E). Thus, our data suggested that disruption of *hif3a* attenuated hypoxia tolerance in zebrafish.

Disruption of *hif3a* in zebrafish reduced erythrocytes

When we routinely examined the *hif3a*$^{+/+}$ and *hif3a*$^{-/-}$ larvae under a dissection microscope, we noticed that the *hif3a*$^{-/-}$ larvae always had fewer blood cells compared with *hif3a*$^{+/+}$ larvae. Given the importance of red blood cells for hypoxia tolerance (Bigham and Lee, 2014; Lee and Percy, 2011; Lorenzo et al., 2014; Sun et al., 2017), we measured the red blood cells of *hif3a*$^{+/+}$ and *hif3a*$^{-/-}$ embryos using o-Dianisidine staining. At 36 h post fertilization (hpf), there were fewer o-Dianisidine-positive cells in the *hif3a*$^{-/-}$ embryos than in the *hif3a*$^{+/+}$ embryos (Fig. 2A,B). Gata1 is an erythroid-specific transcription factor that is essential for erythropoiesis, and Tg(*gata1*:eGFP) zebrafish are widely used for monitoring living red blood cells (de Jong and Zon, 2005; Ferreira et al., 2005; Long et al., 1997; Lyons et al., 2002). To validate our observed phenotype, we mated Tg(*gata1*:eGFP) zebrafish with *hif3a*$^{-/-}$, generating Tg(*gata1*:eGFP)/*hif3a*$^{+/+}$ and Tg(*gata1*:eGFP)/*hif3a*$^{-/-}$. From 24-48 hpf, we observed fewer *gata1*-positive cells in the *hif3a*$^{-/-}$ than in their WT siblings (Fig. 2C,D). These data suggest that knockout of *hif3a* disrupts erythropoiesis in zebrafish.

Reduced hypoxia tolerance was not only exhibited by the *hif3a*$^{-/-}$ larvae (Fig. 1A,B,D), but also by the *hif3a*$^{-/-}$ adults (Fig. 1C; Movie 2). Thus, we examined erythrocyte numbers in adult. As it is difficult to measure total erythrocytes in each adult, we used relative erythrocyte number (the number of cells counted in a given blood volume) to compare *hif3a*$^{+/+}$ and *hif3a*$^{-/-}$ adults. Consistently, *hif3a*$^{-/-}$ had fewer erythrocytes than *hif3a*$^{+/+}$ (Fig. 2E).

To determine whether the defective erythropoiesis displayed by the *hif3a*$^{-/-}$ was associated with erythroid maturation, we analyzed the morphology of isolated red blood cells using May-Grunwald-Giemsa staining (Fig. 2F,G; De La Garza et al., 2016). *hif3a*$^{-/-}$ had a higher percentage of proerythroblasts and a lower percentage of mature erythroid precursors at 2 days post fertilization (dpf) than in the WT (Fig. 2F). The relative level of proerythroblasts decreased in the *hif3a*$^{-/-}$ at 5 dpf, but remained higher than the level in their WT siblings (Fig. 2G). These data suggested that the deletion of *hif3a* might impede erythroid cell maturation, resulting in fewer mature red blood cells in *hif3a*$^{-/-}$ embryos.

To determine whether loss of one copy of *hif3a* can affect red blood cells and survival rate, we also compared the red blood cells among *hif3a*$^{+/+}$, *hif3a*$^{+/-}$ and *hif3a*$^{-/-}$ embryos using o-Dianisidine staining. No significant difference was detected between *hif3a*$^{+/+}$and *hif3a*$^{+/-}$ (Fig. S2F). In agreement with this, under hypoxia, the death curve was similar between *hif3a*$^{+/+}$and *hif3a*$^{+/-}$ (Fig. S2G).

Disruption of zebrafish *hif3a* abrogated the expression of hematopoietic marker genes, and ectopic expression of *hif3a* mRNA rescued hematopoiesis defects in *hif3a*$^{-/-}$ zebrafish

To figure out the mechanisms of *hif3a* on erythropoiesis, we examined the expression of hematopoietic markers using whole mount *in situ* hybridization. *scl* (*tal1*) and *lmo2* are two primitive progenitor cell marker genes in zebrafish hematopoiesis (de Jong and Zon, 2005). At the 10-somite stage, no significant difference was detected in expression levels of *scl* and *lmo2* between *hif3a*$^{+/+}$ and *hif3a*$^{-/-}$ (Fig. S3A). *MyoD* staining (the somatic mesoderm marker) at the 14-somite stage indicated that overall embryogenesis was not influenced by disruption of *hif3a* (Fig. S3B). However, at 24 hpf, *gata1* expression was dramatically reduced in *hif3a*$^{-/-}$ embryos compared with *hif3a*$^{+/+}$ embryos. Consistently, the expression levels of *alas2* (a key enzyme for heme biosynthesis) and *band3* (*slc4a1a*; an erythroid-specific cytoskeletal protein)

Development (2020) 147, dev185116. doi:10.1242/dev.185116

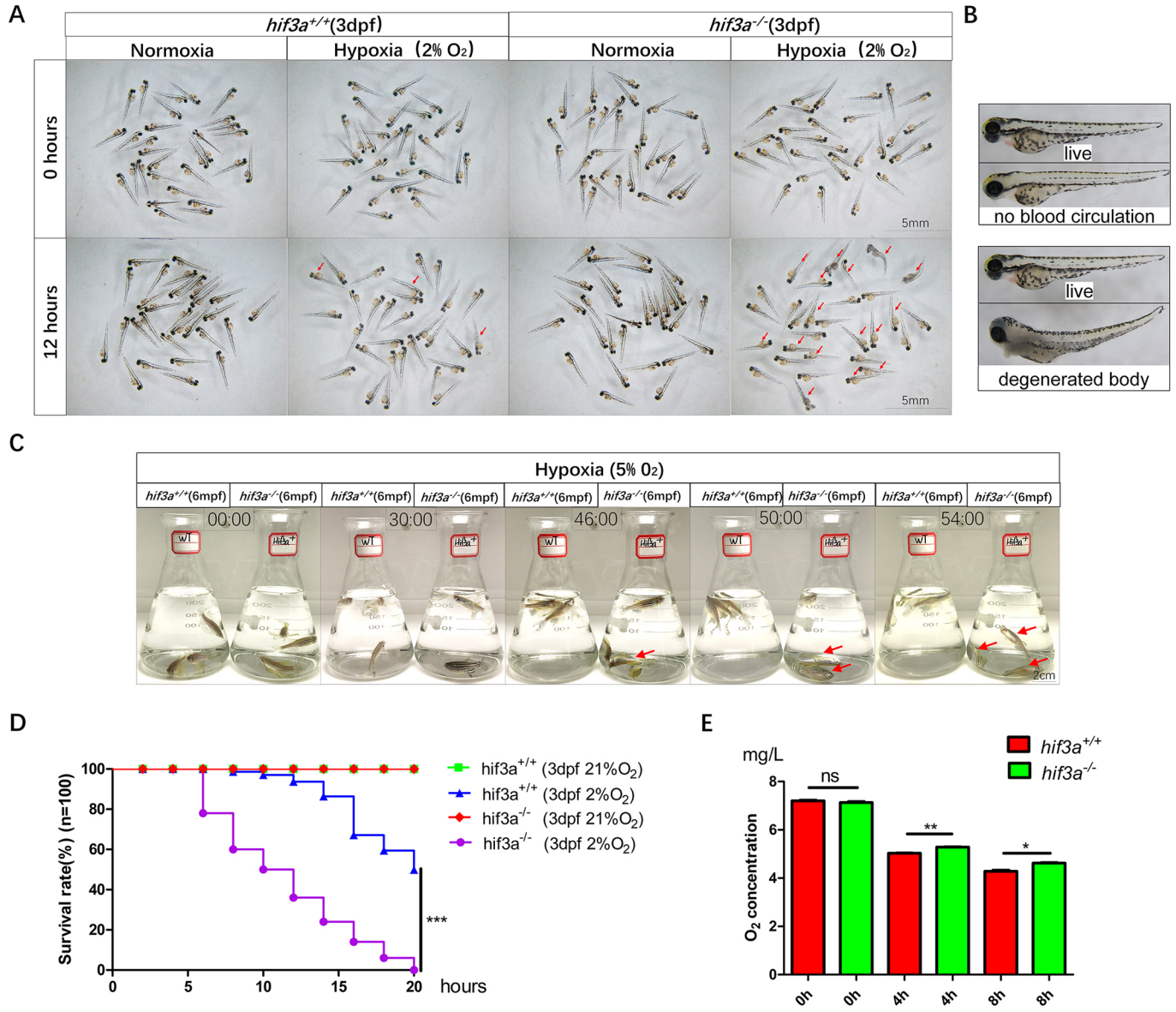

Fig. 1. Zebrafish *hif3a* facilitates hypoxia tolerance. (A) Representative images of *hif3a*$^{-/-}$ larvae and WT (*hif3*$^{+/+}$) larvae (30 larvae for each, 90 larvae in total; 3 dpf), subjected to normoxia (21% O_2) or hypoxia (2% O_2) for 12 h. The dead larvae (marked by red arrows) exhibited lack of movement, absence of blood circulation and bodily degeneration. (B) Representative images of living and dead zebrafish larvae. (C) *Hif3a*$^{-/-}$ adults were more sensitive to hypoxia (5% O_2) compared with their WT siblings. Survival of *hif3a*$^{+/+}$ (left flask) and *hif3a*$^{-/-}$ (right flask) (6 mpf) after 0 min, 30 min, 46 min, 50 min and 54 min in hypoxic conditions (5% O_2) (three zebrafish for each, three replicates). Red arrows indicate dying zebrafish. (D) The survival rate curve of *hif3a*$^{-/-}$ larvae and their WT siblings. The oxygen concentration of the hypoxia workstation was adjusted to 2% before experimentation. The dead larvae were counted once every two hours (100 larvae). (E) Oxygen consumption rate was lower in *hif3a*$^{-/-}$ than in their WT siblings (6 mpf). The experiments were repeated at least three times. Error bars indicate s.e.m.; ns, not significant; **P*<0.05; ***P*<0.01; ****P*<0.001 (unpaired, two-tailed Student's *t*-test).

were reduced in *hif3a*$^{-/-}$ at 24 hpf (Fig. 3A; Brownlie et al., 1998; Paw et al., 2003). In addition, the expression levels of *hbae1*, *hbae3* and *hbbe1* (three erythrocyte-specific hemoglobin genes), were reduced in *hif3a*$^{-/-}$ at 48 hpf compared with *hif3a*$^{+/+}$ (Fig. 3B). The downregulation of *gata1* expression in *hif3a*$^{-/-}$ at 24 hpf was confirmed with quantitative RT-PCR assays (qRT-PCR) (Fig. S4A). The decreased expression levels of *alas2*, *band3*, *hbae1*, *hbae3* and *hbbe1* in *hif3a*$^{-/-}$ compared with *hif3a*$^{+/+}$ were also confirmed by qRT-PCR assays (Fig. S4A,B).

Murine models suggest that *Runx1* and *c-myb* are important factors for adult erythropoiesis (Ferreira et al., 2005). Based on the erythrocyte reduction we observed in adult *hif3a*$^{-/-}$, we sought to determine whether *runx1* and *c-myb* were also downregulated in adult *hif3a*$^{-/-}$. Surprisingly, *runx1* and *c-myb* (*myb*) were upregulated, not downregulated, in the kidneys of adult *hif3a*$^{-/-}$ compared with *hif3a*$^{+/+}$ (Fig. S4C). These results suggest that *hif3a* might not induce *runx1* and *c-myb* expression, and that the decreased erythrocytes in adult *hif3a*$^{-/-}$ might not be because of the effects of *runx1* and *c-myb*.

The glycoprotein hormone erythropoietin (Epo), which is induced by Hifα, regulates red blood cell mass, connecting the hypoxia signaling pathway with erythropoiesis (Lee and Percy, 2011). To determine whether *hif3a* modulates adult erythropoiesis by regulating *epo* (*epoa*), similar to the behavior of *hif1a* and *hif2a*, we measured *epo* expression in adult zebrafish kidneys. Unexpectedly, *epo* expression was upregulated, not downregulated, in *hif3a*$^{-/-}$

Development (2020) 147, dev185116. doi:10.1242/dev.185116

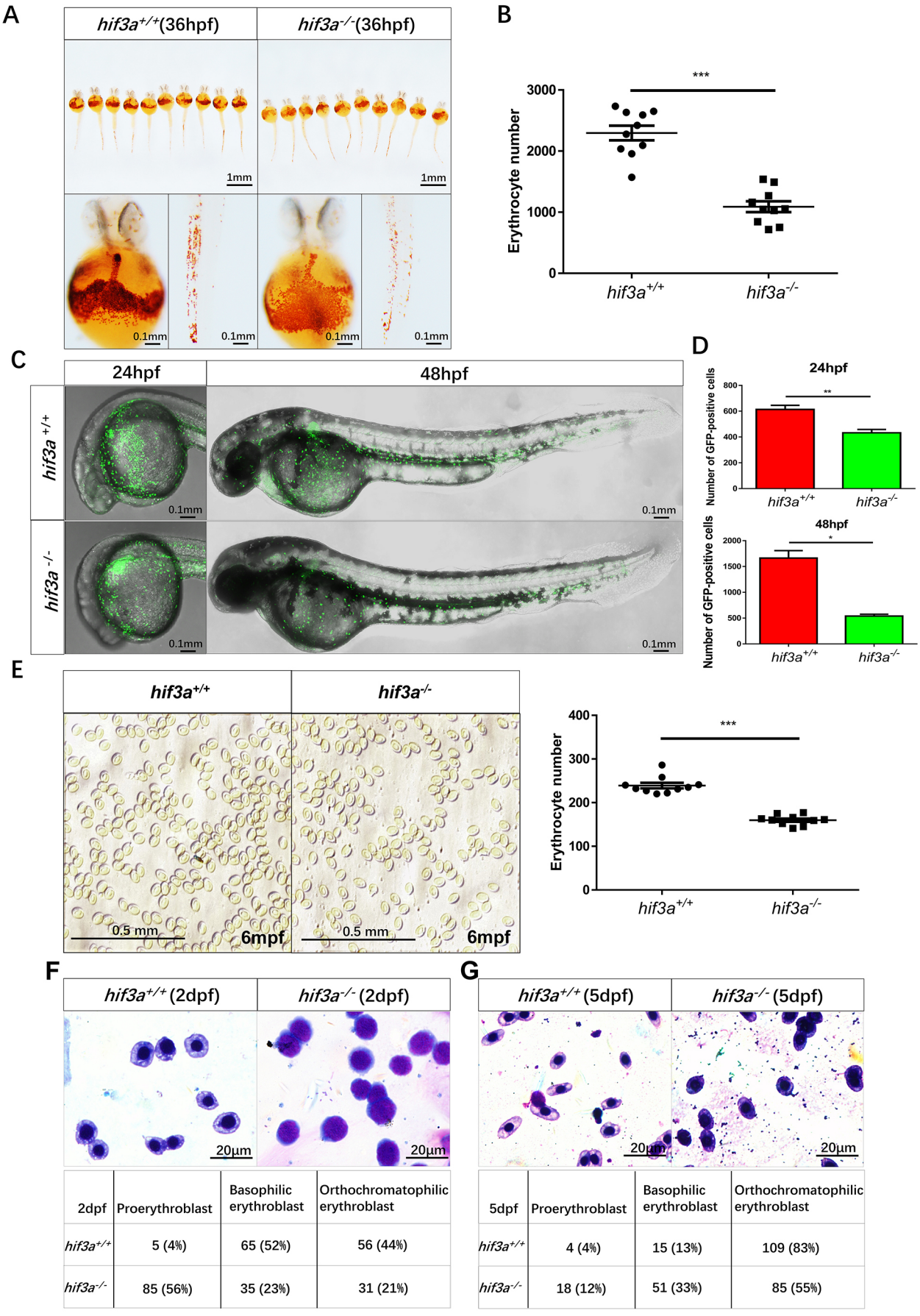

2dpf	Proerythroblast	Basophilic erythroblast	Orthochromatophilic erythroblast
hif3a$^{+/+}$	5 (4%)	65 (52%)	56 (44%)
hif3a$^{-/-}$	85 (56%)	35 (23%)	31 (21%)

5dpf	Proerythroblast	Basophilic erythroblast	Orthochromatophilic erythroblast
hif3a$^{+/+}$	4 (4%)	15 (13%)	109 (83%)
hif3a$^{-/-}$	18 (12%)	51 (33%)	85 (55%)

Fig. 2. See next page for legend.

Development (2020) 147, dev185116. doi:10.1242/dev.185116

Fig. 2. The number of erythrocytes is reduced and primitive erythroid maturation is retarded in *hif3a*$^{-/-}$. (A) O-Dianisidine staining of functional hemoglobin in the mature primitive erythrocytes in *hif3a*$^{+/+}$ (left) and *hif3a*$^{-/-}$ (right) at 36 hpf. The experiments were repeated three times. (B) The number of erythrocytes was reduced in *hif3a*$^{-/-}$ (10 larvae). (C) Fluorescent images of Tg(*gata1*:eGFP)/*hif3a*$^{+/+}$ (top) and Tg(*gata1*:eGFP)/*hif3a*$^{-/-}$ (bottom) indicated that *hif3a*$^{-/-}$ have fewer *gata1*-positive erythrocytes at 24 hpf and 48 hpf. (D) Quantitation of *gata1*-positive erythrocytes in Tg(*gata1*:eGFP)/*hif3a*$^{+/+}$ and Tg(*gata1*:eGFP)/*hif3a*$^{-/-}$ at 24 hpf (top) and 48 hpf (bottom) (10 larvae for each, three replicates). (E) The number of erythrocytes was significantly reduced in *hif3a*$^{-/-}$ compared with *hif3a*$^{+/+}$ at 6 mpf. Representative image of erythrocytes in the counting chamber (1 mm×1 mm) (right); scatter plot indicates erythrocyte numbers in 10 counting chambers (left). (F,G) Representative images of May–Grunwald–Giemsa-stained erythroblasts in *hif3a*$^{+/+}$ and *hif3a*$^{-/-}$ larvae at 2 dpf (F) and 5 dpf (G). Cells were morphologically classified at various stages of maturation; numbers (and percentages in brackets) of *hif3a*$^{+/+}$ and *hif3a*$^{-/-}$ larvae at each stage are shown. Error bars indicate the s.e.m.; **P*<0.05; ***P*<0.01; ****P*<0.001 (unpaired, two-tailed Student's *t*-test).

compared to *hif3a*$^{+/+}$ (Fig. S4C). To further determine whether the modulation of erythropoiesis by *hif3a* is indeed independent of Epo, we examined the effect of micro-injection of *epo* mRNA on erythropoiesis in *hif3a*$^{-/-}$ embryos. Of note, micro-injection of *epo* mRNA could not rescue the defects of erythropoiesis in *hif3a*$^{-/-}$ embryos (Fig. S5). These data suggested that *hif3a* might not modulate erythropoiesis by directly regulating *epo* expression.

To further confirm that erythropoiesis defects of *hif3a*$^{-/-}$ were specifically due to silencing of *hif3a*, we microinjected synthesized *hif3a* mRNA into *hif3a*$^{-/-}$ embryos at the one-cell stage. Expression of microinjected *hif3a* mRNA was confirmed (Fig. S6A). We then examined red blood cells using o-Dianisidine staining, and quantified marker gene expression using whole-mount *in situ* hybridization (WISH) and qRT-PCR assays. At 36 hpf, embryos microinjected with *hif3a* mRNA had more red blood cells than embryos microinjected with GFP-mRNA (Fig. 3C). Consistently, the expression levels of *gata1*, *alas2*, *band3*, *hbae1*, *hbae3* and *hbbe1* were higher in the *hif3a*$^{-/-}$ embryos microinjected with *hif3a* mRNA compared with the *hif3a*$^{-/-}$ embryos microinjected with GFP-mRNA (Fig. 3D,E; Fig. S6B,C).

These data suggest that the disruption of zebrafish *hif3a* abrogated the expression of hematopoietic marker genes, resulted in defects of erythropoiesis; and that *gata1* might be the downstream effector mediating the function of *hif3a* in erythropoiesis.

Zebrafish have two waves of hematopoiesis, primitive hematopoiesis (embryonic hematopoiesis) and definitive hematopoiesis (adult hematopoiesis) (de Jong and Zon, 2005; Paik and Zon, 2010). *gata1* is crucial for both primitive and definitive erythropoiesis (Ferreira et al., 2005). In this study, we found that *gata1* was downregulated in *hif3α*$^{-/-}$, which correlated well with the reduction of erythrocytes in *hif3α*$^{-/-}$. Therefore, *gata1* might be the main target by which *hif3α* mediates erythropoiesis.

Hif3α activated *gata1* expression by recognizing the HRE site located in the *gata1* promoter

Although the function of mammalian HIF3α is debatable due to the complexity of the splicing isoforms, zebrafish Hif3α serves as an oxygen-dependent transcription factor (Zhang et al., 2016). We observed that erythroid cell maturation was retarded and *gata1* expression was reduced during erythropoiesis in *hif3a*$^{-/-}$ zebrafish. Therefore, we attempted to determine whether zebrafish Hif3α acted as a transcription factor to regulate *gata1* expression. Initially, we examined expression patterns of *hif3a* and *gata1* in adult zebrafish tissues (3 mpf) as well as at different developmental stages. *hif3a* was highly expressed in kidney, and *gata1* was highly expressed in spleen and kidney (Fig. 4A,B), indicating a correlation expression pattern between *hif3a* and *gata1* in tissues. Intriguingly, during development *hif3a* expression reached its highest level from 12-16 hpf, *gata1* expression started to increase from 12 hpf and reached its highest level at 16 hpf (Fig. 4C,D), further implying an intrinsic connection between *hif3a* and *gata1* expression.

Subsequently, we examined whether Hif3α had transcriptional activity using an artificial luciferase reporter assay system in embryos (Zhou et al., 2009). Hif3α indeed had transcriptional activity (Fig. 4E). Subsequently, we prepared a series of deletion and mutation constructs for the zebrafish *gata1* promoter luciferase reporter (Fig. 4F). Overexpression of *hif3a* significantly activated the *gata1* promoter luciferase constructs, −1380-+1580, −890-+1580, −406-+1580 and −164-+1580 in EPC cells (Fig. 4G). However, when a potential HRE (GCGTG) located at −105-−101 was mutated (GAAAG) (Fig. 4F), the promoter luciferase reporter (−406-+1580/HRE mutant) was not activated by overexpression of *hif3a* in EPC cells (Fig. 4H). Further chromatin-immunoprecipitation (ChIP) assays using anti-Hif3α antibody (Zhang et al., 2012) indicated that Hif3α could bind to the *gata1* promoter-containing HRE site (Fig. 4I).

In addition to *hif3a*, another splicing alternative isoform is known in zebrafish: *hif3a*2 (Duan, 2016; Zhang et al., 2016). Disruption of *hif3a* at two loci also generated two novel peptides (M1 and M2) (Fig. S2B). To determine whether these three proteins affected *gata1* induction, we performed promoter assays. Interestingly, overexpression of these three proteins did not activate the *gata1* promoter (Fig. S7A-C). These findings not only suggested that *hif3a* plays a specific role for *gata1* induction, but also indicated that the knockout of *hif3a* at two loci completely disrupted *hif3a* function in zebrafish.

In the mutant M2 (*hif3a*$^{ihb20180621/ihb20180621}$), we confirmed that the expression levels of *gata1*, *alas2*, *hbae1* and *hbbe1* were reduced compared with WT siblings (*hif3a*$^{+/+}$) (Fig. S8A,B). Thus, our results suggested that zebrafish *hif3a* directly activated *gata1* expression by recognizing the HRE site located in the promoter of *gata1*.

Whether HIF3α acts as a dominant negative transcriptional regulator of HIF1α and/or HIF2α, or acts as a transcription factor in response to hypoxia, is largely dependent upon the variant and the biological model, particularly in mammals (Heikkilä et al., 2011; Makino et al., 2007; Maynard et al., 2005). However, in zebrafish, Hif3α binds to the promoter sequences of several genes, and induces the expression of these genes under hypoxic conditions (Zhang et al., 2014). Here, we provide additional evidence supporting that zebrafish Hif3α serves as a transcription factor to induce *gata1* expression.

As reported previously, Hif3α is degraded during normoxia in zebrafish (Zhang et al., 2014). However, in this study we observed that defects of erythropoiesis in *hif3a*$^{-/-}$ zebrafish were steady-state. We sought to determine whether Hif3α protein stability was also steady-state from embryos to adult tissues. Using western blot analysis, we confirmed that Hif3α protein was stable from embryos to adult tissues (Figs S1E and S9).

In addition, we noticed that disruption of *hif3a* enhanced expression of *hif1ab* and *hif2ab*, suggesting some redundant functions between *hif3a and hif1a/hif2a* in zebrafish (Fig. S10A,B). Consistent with this notion, the *hif1a* downstream targets *glut1* and *pdk1*, and the *hif2a* downstream targets *pou5f1* and *pai1* were increased in *hif3a*$^{-/-}$ larvae (Fig. S10C-F).

Given the well-known role of *hif1a* in regulating erythropoiesis (Semenza, 2009), we intended to determine whether microinjection of *hif1ab* mRNA could rescue the defects of erythropoiesis in

Development (2020) 147, dev185116. doi:10.1242/dev.185116

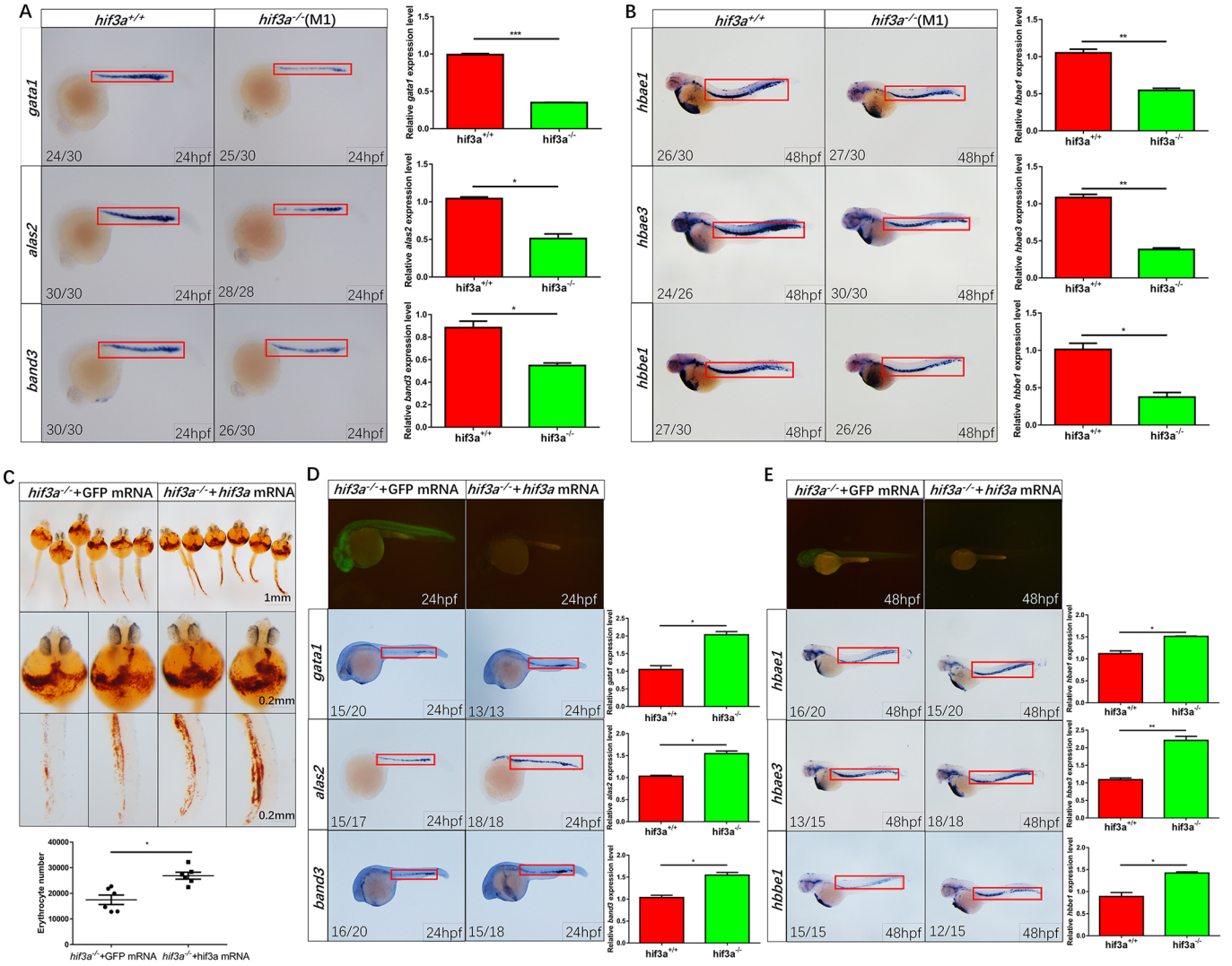

Fig. 3. Disruption of *hif3a* influences expression of hematopoietic marker genes, but ectopic expression of *hif3a* partially rescues hematopoietic defects exhibited in *hif3a*$^{-/-}$. (A) Expression levels of the erythrocytic markers *gata1*, *alas2* and *band3* were reduced significantly in *hif3a*$^{-/-}$ larvae at 24 hpf. Quantitation of the signal in the red rectangle is shown on the right (10 larvae for each, three replicates). (B) Expression levels of the erythrocyte-specific hemoglobin markers *hbae1*, *hbae3* and *hbbe1* were reduced in *hif3a*$^{-/-}$ larvae at 48 hpf. Quantitation of the signal in the red rectangle shown on the right (10 larvae for each, three replicates). (C) O-Dianisidine staining indicated that co-injection of *hif3a* mRNA partially restored hemoglobin levels in *hif3a*$^{-/-}$ larvae compared with co-injection of GFP mRNA at 36 hpf. *Hif3a* and GFP mRNA, 750 pg/embryo. Quantitation showed in the bottom panel (six larvae for each, three replicates). (D) Expression levels of the erythrocytic markers *gata1*, *alas2* and *band3* were restored by injection of *hif3a* mRNA in *hif3a*$^{-/-}$ embryos as compared to the injection of the GFP mRNA control at 24 hpf. Quantitation of the signal in the red rectangle is shown on the right (10 larvae for each, three replicates). (E) Expression levels of the erythrocytic markers *hbae1*, *hbae3* and *hbbe1*, were restored by injection of *hif3a* mRNA in *hif3a*$^{-/-}$ embryos as compared to the injection of the GFP mRNA control at 48 hpf. Quantitation of the signal in the red rectangle is shown on the right (10 larvae for each, three replicates). The number of stained embryos is indicated in the left lower corner of each representative picture. M1, mutant 1. Error bars indicate the s.e.m.; **P*<0.05; ***P*<0.01; ****P*<0.001 (unpaired, two-tailed Student's *t*-test).

hif3a$^{-/-}$ embryos. Based on o-Dianisidine staining of embryos, microinjection of *hif1ab* mRNA could partially restore the defects of erythropoiesis in *hif3a*$^{-/-}$ embryos (Fig. S10G-I). Furthermore, we found that the red blood cell numbers were partially recovered and their maturation was obviously fixed after microinjection of *hif1ab* mRNA (Fig. S10J-M), which seemed to rely on *gata1* upregulation because *gata1* expression was indeed increased (Fig. S10N,O).

In this study, we noticed that disruption of *hif3a* could cause redundant upregulation of *hif1ab*. It appeared that microinjection of *hif1ab* mRNA could induce *gata1* upregulation, resulting in partially rescuing defects of erythropoiesis in *hif3a*$^{-/-}$ embryos. However, disruption of *hif3a* in zebrafish eventually caused defects of erythropoiesis. Therefore, the direct upregulation of *gata1* by Hif3α might account for a main mechanism of Hif3α in modulating erythropoiesis of zebrafish.

Given the well-known role of Phd enzymes and VHL proteins in regulating HIF activity and the similarity between HIF1α, HIF2α and HIF3α, we sought to determine whether zebrafish *phd2a*, *phd2b*, *phd3* and *vhl* have effects on *hif3a* activity. We performed promoter assays and western blot analysis. Co-expression of *phd2a*, *phd2b*, *phd3* and *vhl* decreased the activity of HRE luciferase reporter and *gata1* promoter reporter induced by Hif3α (Fig. S11A,B). As expected, co-expression of *phd2a*, *phd2b*, *phd3* and *vhl* also caused Hif3α protein degradation (Fig. S11C). These data suggest that Hif3α might behave similar to Hif1α and Hif2α in the hypoxia signaling pathway.

Development (2020) 147, dev185116. doi:10.1242/dev.185116

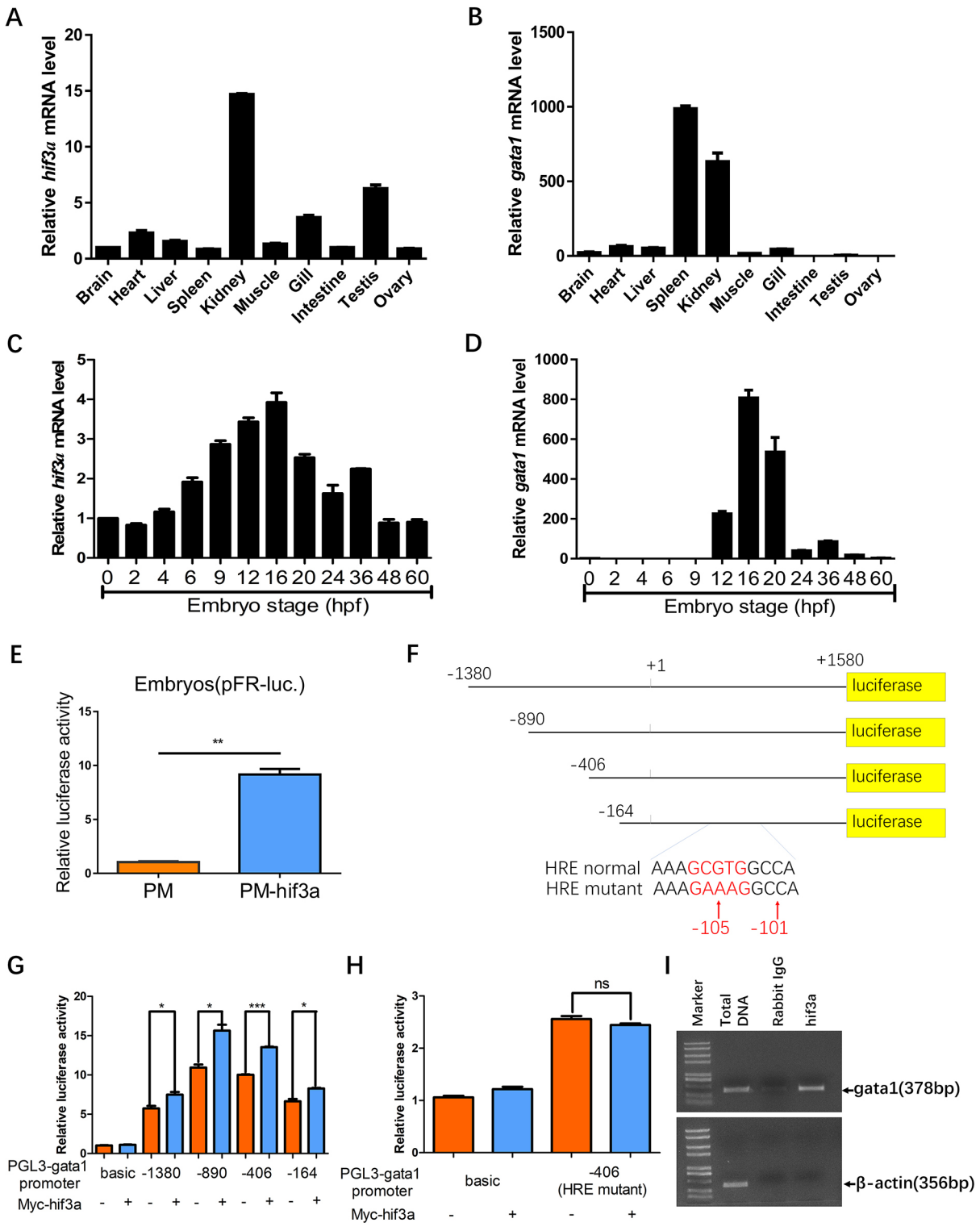

Fig. 4. *Hif3a* activates *gata1* expression by directly binding to and recognizing the HRE site located in the *gata1* promoter. (A) Expression pattern of *hif3a* in zebrafish tissues (three adults; 3 mpf). (B) Expression pattern of *gata1* in zebrafish tissues (three adults; 3 mpf). (C) Expression pattern of *hif3a* at different developmental stages (30 embryos). (D) Expression pattern of *gata1* at different developmental stages (30 embryos). (E) Luciferase reporter assays indicate that *hif3a* has transcriptional activity (50 embryos). PM/PM-hif3a, 37.5 pg/embryo; pFR, 28.1 pg/embryo; PTK, 25 pg/embryo. (F) Schematic of different deletion constructs of the *gata1* promoter luciferase reporter. (G) Luciferase reporter assays for different deletion constructs of the *gata1* promoter in the presence or absence of myc-Hif3α in EPC cells. ['+1' is designated as the transcription initiation site; the translation starting site (ATG code) is located at '+1580']. (H) When the potential HRE site located in the *gata1* promoter was mutated, the induction of *gata1* promoter activity by *hif3a* was lost in EPC cells. + indicates that the components of the expression vectors have been transfected, – indicates that the components of the expression vectors have not been transfected. Values graphed are the means of three independent experiments performed in triplicate. (I) ChIP assay using anti-Hif3α antibody showed that Hif3α binds to the promoter of *gata1* directly in zebrafish embryos (~700 embryos for each, three replicates; 24 hpf). qRT-PCR experiments were repeated three times. Error bars indicate s.e.m.; ns, not significant; **P*<0.05; ***P*<0.01; ****P*<0.001 (unpaired, two-tailed Student's *t*-test).

Development (2020) 147, dev185116. doi:10.1242/dev.185116

MATERIALS AND METHODS

Generation of *hif3a*-null zebrafish

We used CRISPR/Cas9 to knock out *hif3a* in zebrafish (*Danio rerio*). First, *hif3a* sgRNA was designed using the CRISPR design tool (http://crispr.mit.edu). The zebrafish codon Optimized Cas9 plasmid (provided by Dr Bo Zhang, Peking University, China) was digested using XbaI, then purified and transcribed using the T7 mMessage mMachine Kit (Ambion). We used a PUC9 gRNA vector (provided by Dr Bo Zhang, Peking University, China) to amplify the *hif3a* sgRNA template. The primers used to amplify *hif3a* sgRNA were: forward primer 1 (mutant 1), 5′-GTAATACGACTCACTA-TAGGACAAAGCTGCCATCATGAGTTTTAGAGCTAGAAATAGC-3′; forward primer 2 (mutant 2), 5′-GTAATACGACTCACTATAGGTGGTG-TTATTTCACTCTGGTTTTAGAGCTAGAAATAGC-3′; and the reverse primer 5′-AAAAGCACCGACTCGGTGCC-3′. SgRNA was synthesized using the Transcript Aid T7 High Yield Transcription Kit (Fermentas).

We injected zebrafish embryos at the one-cell stage (generated as described above) with 1 ng Cas9 RNA and 0.15 ng sgRNA per embryo. The mutations were initially detected using a heteroduplex mobility assay (HMA) as previously described (Cai et al., 2018). Briefly, a short fragment that included the target site was amplified from genomic DNA and two-step PCR was carried out as follows: 95°C for 2 min, and 40 cycles of 95°C for 10 s, 55°C for 30 s and 72°C for 30 s. PCR amplicons were electrophoresed on 15% polyacrylamide gels for 30 min. If the HMA results were positive, the remaining embryos were raised to adulthood as the F0 generation, and were then backcrossed with WT zebrafish (strain AB) to generate the F1 generation. F1s were genotyped with HMAs. Genotype was confirmed by sequencing target sites. Heterozygous F1s were back-crossed with WT zebrafish (strain AB; disallowing offspring-parent matings) to generate the F2 generation. F2 adults carrying the target mutation were inter-crossed to generate F3 offspring. The F3 generation contained WT (+/+), heterozygous (+/−) and homozygous (−/−) individuals. The primers used to identify mutants were: forward primer 1 (mutant 1), 5′-AGTTTGGAGCAGCGGAAG-3′; reverse primer 1 (mutant 1), 5′-AGCATTAGGACATTATGCAGGT-3′; forward primer 2 (mutant 2), 5′-CGAAAGGACAGTCAGAGGTAGA-3′; and reverse primer 2 (mutant 2), 5′-ACCGTTTCCTAGAATTACTGGTTAG-3′. The two novel mutants were named following zebrafish nomenclature guidelines, *hif3a*$^{ihb20180620/ihb20180620}$ (http://zfin.org/ZDB-ALT-180620-1) and *hif3a*$^{ihb20180621/ihb20180621}$ (http://zfin.org/ZDB-ALT-180620-2).

Zebrafish maintenance and cell culture

Zebrafish strain AB, as well as the transgenic line Tg(gata1:EGFP) (provided by Tingxi Liu, Shanghai Institutes for Biological Sciences, Chinese Academy of Sciences, China) were raised, maintained and staged according to standard protocols. EPC cells originally obtained from the American Type Culture Collection were cultured in M199 medium supplemented with 10% fetal bovine serum, maintained at 28°C in a humidified incubator containing 5% CO_2. EPC cells were transfected with the constructed plasmids using VigoFect (Vigorous Biotechnology) following the manufacturer's instruction. pTK-*Renilla* (Promega) was used as an internal control. After transfection, the luciferase activity was measured using the dual-luciferase reporter assay kit following the manufacturer's instruction (Promega).

Hypoxia treatment

The Ruskinn Invivo2 I-400 workstation was used for hypoxia treatment of zebrafish (larvae and adults). The O_2 concentration was adjusted to the appropriate value (2% for larvae and 5% for adults) before experimentation. In our previous studies, we noted that the body weight of adult zebrafish significantly affected hypoxia tolerance (Cai et al., 2018). Therefore, we selected adult zebrafish (at 3 and 6 mpf) with similar body weights (0.32 ±0.02 g; 0.65±0.02 g) for the hypoxia tolerance tests.

For the hypoxia treatments of zebrafish larvae, *hif3a*-null and WT zebrafish were placed into a 10 cm cell culture dish filled with 30 ml of water. The oxygen concentration in the Ruskinn INVIVO2 I-400 workstation was adjusted to 2% ahead of time. Each experiment was repeated three times.

WISH and o-Dianisidine staining

WISH was performed as described previously (Hu et al., 2014). Probes for *scl*, *lmo2*, *gata1*, *myoD*, *alas2*, *band3*, *hbae1*, *hbae3* and *hbbe1* were amplified from the cDNA pool using the primers.

O-Dianisidine staining for hemoglobin was performed as previously described (Hu et al., 2014). Live embryos were soaked in o-Dianisidine staining solution (0.6 mg/ml o-Dianisidine, 166ul 3 M ammonium acetate, 20 ml absolute ethyl alcohol, 30 ml ddH_2O) for 15 min in the dark.

The software IpWin32 was used for quantifying the erythrocyte numbers, GFP-positive cell numbers and gene expression levels in WISH staining. The cell numbers and gene expression levels were measured from the field of view with a same square, and different larvae were chosen for counting (n=3).

Luciferase reporter assays and transcriptional activity assays

EPC cells were seeded in 24-well plates and transfected with the indicated plasmids together with zebrafish *gata1* promoter luciferase reporters and pTK-*Renilla* as an internal control. Luciferase activity was measured 20-24 h after transfection using the Dual-luciferase Reporter Assay System (Promega). For embryos, the plasmids were injected into the embryos at the one-cell stage. About 30 embryos were harvested at 10 hpf and homogenized in Passive Lysis Buffer (Promega). Each experiment was conducted in triplicate and repeated at least three times.

May–Grunwald–Giemsa staining

The embryos (2 dpf and 5 dpf) were placed in 1× PBS dropped on glass slides. The blood cells were released by puncturing the pericardial sac and upper yolk sac of embryos with fine forceps. The slides were air dried at room temperature before staining. The blood cells were stained with May–Grunwald-Giemsa solution 1 (100 µl; ServiceBio) for 5 min, briefly rinsed in purified water, and then stained with May–Grunwald-Giemsa solution 2 (200 µl) for 10 min and briefly rinsed with purified water. Once the slides were dry, a drop of neutral resin was added. Subsequently, the slides were covered with slips and dried overnight. The stained blood cells were visualized and photographed under a 100× oil-immersion lens.

Erythrocyte number counting in adult zebrafish

Adult zebrafish (n=3 for *hif3a*$^{+/+}$ and *hif3a*$^{-/-}$; 6 mpf; body weight=0.63± 0.01 g) were skin-dried carefully using filter paper and dissected near to the heart region using an eye scissor. Approximately 15 µl blood was collected from the beating heart using a syringe infiltrated with heparin in advance. Subsequently, 1 µl blood was mixed with 99 µl phosphate-buffered saline (PBS) in 1.5 ml EP tube. Then 10 µl diluted blood was added into a hemocytometer for counting the erythrocyte number. The erythrocytes in 10 chambers (1mm×1 mm) were counted under an inverted microscope (BX53, Olympus) for each zebrafish. Each zebrafish was counted three times in a randomly selected different field. Simultaneously, the blood cell pictures were photographed for reference.

qRT-PCR

Total RNAs were extracted from embryos or kidneys using the TRIzol reagent (Invitrogen), and the first-strand cDNA synthesis kit (Fermentas) was used to synthesize cDNA. qRT-PCR assays were performed using MonAmp™ SYBR® Green qPCR Mix (high Rox) (Monad Bio.). The primers used for RT-PCR were: *hif3a, 5′-GCTGGATGGCTTGTCTGAT-GG-3′ and 5′-CCCTCATGAGAGCTGCTGTG-3′; gata-1*, 5′-GAGACTG-ACCTACTGCCATCG-3′ and 5′-TCCCAGAATTGACTGAGATGAG-3′; *alas2*, 5′-GCAAAATGGCCTTCTCCCTC-3′ and 5′-TCAAACCTGAG-GTGTCTTGG-3′; *band3*, 5′-GTGATGGTTGGTGTCTCAAT-3′ and 5′-TAGTTGGCACACGGGTGACA-3′; *hbae1*, 5′-CTCTCTCCAGGAT-GTTGATT-3′ and 5′-GGGACAGAATCTTGAAATTG-3′; *hbae3*, 5′-CT-CTTTCCAGGACTTTGTTC-3′ and 5′-GGTTGATGATCTTGAAGTTT-3′; *hbbe1*, 5′-ATGGTTGCTGCCCACGGTAA-3′ and 5′-CAGCCAAAA-G-CCTGAAGTTG-3′; *β-actin*, 5′-TACAATGAGCTCCGTGTTGC-3′ and 5′-ACATACAATGGCAGGGGTGTT-3′; *runx*, 5′-GGGACGCCAAATA-CGAACCT-3′ and 5′-GCAGGACGGAGCAGAGGAAG-3′; *c-myb*, 5′-AGTTACTTCCGGGAAGAACCG-3′ and 5′-AGAGCAAGTGGAA-ATGGCACC-3′; *epo*, 5′-GTGCCTCTCACTGAGTTCTTGGAAG-3′ and 5′-CTCGTTCAGCATGTGTAAGCCTGAC-3′. *β-actin* was used as internal controls. Applied Biosystems Step One was used for data collection.

Development (2020) 147, dev185116. doi:10.1242/dev.185116

Oxygen concentration measurement

We measured zebrafish oxygen consumption in 250 ml flasks (n=12), each containing 250 ml water. The oxygen concentration in water was measured using an LDO101 probe (HQ30d, HACH). A total of 12 adult zebrafish with similar weight (n=6 for *hif3a*-null and WT) were used for measurement. We placed each *hif3a*-null or WT zebrafish in an individual flask, and then tightly sealed the flasks with plastic film. After 4 h, we measured the oxygen concentration in each flask (n=6) with the LDO101 probe. After 8 h, we measured the oxygen concentration in the remaining flasks (n=6) using the LDO101 probe.

ChIP assay

We performed ChIP assays using an Enzymatic Chromatin IP Kit (9002s) (Cell Signaling Technology) following the manufacturer's protocol. Briefly, 2000 embryos were harvested at 16 hpf and sonicated. Then, the protein A/G agarose beads (30 µl) (Santa Cruz Biotechnology) were added to each sample and the mixtures were rotated at 4°C for 1 h. Subsequently, the supernatants were incubated with anti-Hif3α antibody (provided by Dr Cunming Duan, University of Michigan, USA) (Zhang et al., 2012) or rabbit IgG (control) (Santa Cruz Biotechnology) and rotated at 4°C overnight. The primers for amplifying the promoter region of *gata1* were: 5′-GTCTATAAGGTCATAT-AGGC-3′and 5′-CTTCAGTCTTTGGGAACTAG-3′. The primers for amplifying *β-actin* were: 5′-ATCATGTTCGAGACCTTCAA-3′ and 5′-TAGC-TCTTCTCCAGGGAGGA-3′.

Erythrocyte number counting in adult zebrafish and quantification of RNA levels in zebrafish embryos

We used Image-Pro Plus software to analyze digital images for counting erythrocyte numbers and quantifying RNA levels. For counting erythrocyte numbers: briefly, a standard color parameter of one cell was set and the rectangular area of interest was used to select region, then, the information object definition parameter was chosen for measuring the signal. For quantifying RNA levels of *in situ* hybridization staining, the RNA signal measured from *in situ* hybridization staining of one control zebrafish was set as '1' initially, the RNA levels in other zebrafish were calculated after being compared with the signal value of control zebrafish.

Erythrocyte number counting in zebrafish larvae (2dpf)

The zebrafish larvae (2 dpf) were placed in 10 µl 1×PBS dropped on glass slides. The blood cells were released by puncturing the pericardial sac and upper yolk sac of embryos with fine forceps, and then mixed with 90 µl PBS in 1.5 ml EP tube. We added 10 µl diluted blood into a hemocytometer for counting the erythrocyte number. The erythrocytes in four chambers (1 mm×1 mm) were counted under an inverted microscope (BX53, Olympus) for each zebrafish (n=5 larvae). Each zebrafish was counted three times in a randomly selected different field. Simultaneously, the blood cell pictures were photographed for reference.

Statistical analysis

GraphPad Prism 7 software was used for all statistical analysis. Differences between experimental and control groups were determined using unpaired two-tailed Student's t-test (where two groups of data were compared). P values less than 0.05 were considered statistically significant. For animal survival analysis, the Kaplan–Meier method was adopted to generate graphs, and the survival curves were analyzed by log-rank analysis.

Acknowledgements

We are grateful to Drs Cunming Duan and Ling Lu for providing anti-Hif3α antibody. We also thank Drs Peter Ratcliffe, Navdeep Chandel, Bo Zhang and Jingwei Xiong for the generous gift of reagents.

Competing interests

The authors declare no competing or financial interests.

Author contributions

Conceptualization: W.X., X.C.; Software: X.C.; Validation: X.C., Z.Z., J.Z.; Formal analysis: W.X., X.C.; Investigation: X.C., Z.Z., J.Z.; Resources: J.Z., Q.L., D.Z., X.L., J.W., G.O.; Data curation: J.Z., D.Z.; Writing - original draft: W.X., X.C.; Writing - review & editing: W.X., X.C.; Visualization: X.C., Z.Z.; Supervision: W.X.; Funding acquisition: W.X.

Funding

W.X. is supported by the Strategic Priority Research Program of the Chinese Academy of Sciences (XDA24010308); the National Natural Science Foundation of China (31830101, 31721005 and 31671315); and the National Key Research and Development Program of China (2018YFD0900602). X.C. is supported by State Key Laboratory of Freshwater Ecology and Biotechnology (2020FB07).

Supplementary information

Supplementary information available online at
https://dev.biologists.org/lookup/doi/10.1242/dev.185116.supplemental

Peer review history

The peer review history is available online at
https://dev.biologists.org/lookup/doi/10.1242/dev.185116.reviewer-comments.pdf

References

Aragonés, J., Fraisl, P., Baes, M. and Carmeliet, P. (2009). Oxygen sensors at the crossroad of metabolism. *Cell Metab.* **9**, 11-22. doi:10.1016/j.cmet.2008.10.001

Augstein, A., Poitz, D. M., Braun-Dullaeus, R. C., Strasser, R. H. and Schmeisser, A. (2011). Cell-specific and hypoxia-dependent regulation of human HIF-3alpha: inhibition of the expression of HIF target genes in vascular cells. *Cell. Mol. Life Sci.* **68**, 2627-2642. doi:10.1007/s00018-010-0575-4

Bigham, A. W. and Lee, F. S. (2014). Human high-altitude adaptation: forward genetics meets the HIF pathway. *Genes Dev.* **28**, 2189-2204. doi:10.1101/gad.250167.114

Bishop, T. and Ratcliffe, P. J. (2015). HIF hydroxylase pathways in cardiovascular physiology and medicine. *Circ. Res.* **117**, 65-79. doi:10.1161/CIRCRESAHA.117.305109

Brownlie, A., Donovan, A., Pratt, S. J., Paw, B. H., Oates, A. C., Brugnara, C., Witkowska, H. E., Sassa, S. and Zon, L. I. (1998). Positional cloning of the zebrafish sauternes gene: a model for congenital sideroblastic anaemia. *Nat. Genet.* **20**, 244-250. doi:10.1038/3049

Cai, X., Zhang, D., Wang, J., Liu, X., Ouyang, G. and Xiao, W. (2018). Deletion of the fih gene encoding an inhibitor of hypoxia-inducible factors increases hypoxia tolerance in zebrafish. *J. Biol. Chem.* **293**, 15370-15380. doi:10.1074/jbc.RA118.003004

de Jong, J. L. O. and Zon, L. I. (2005). Use of the zebrafish system to study primitive and definitive hematopoiesis. *Annu. Rev. Genet.* **39**, 481-501. doi:10.1146/annurev.genet.39.073003.095931

De La Garza, A., Cameron, R. C., Nik, S., Payne, S. G. and Bowman, T. V. (2016). Spliceosomal component Sf3b1 is essential for hematopoietic differentiation in zebrafish. *Exp. Hematol.* **44**, 826-837.e824. doi:10.1016/j.exphem.2016.05.012

Duan, C. (2016). Hypoxia-inducible factor 3 biology: complexities and emerging themes. *Am. J. Physiol. Cell Physiol.* **310**, C260-C269. doi:10.1152/ajpcell.00315.2015

Ferreira, R., Ohneda, K., Yamamoto, M. and Philipsen, S. (2005). GATA1 function, a paradigm for transcription factors in hematopoiesis. *Mol. Cell. Biol.* **25**, 1215-1227. doi:10.1128/MCB.25.4.1215-1227.2005

Greer, S. N., Metcalf, J. L., Wang, Y. and Ohh, M. (2012). The updated biology of hypoxia-inducible factor. *EMBO J.* **31**, 2448-2460. doi:10.1038/emboj.2012.125

Gu, Y. Z., Moran, S. M., Hogenesch, J. B., Wartman, L. and Bradfield, C. A. (1998). Molecular characterization and chromosomal localization of a third alpha-class hypoxia inducible factor subunit, HIF3 alpha. *Gene Expr.* **7**, 205-213.

Hara, S., Hamada, J., Kobayashi, C., Kondo, Y. and Imura, N. (2001). Expression and characterization of hypoxia-inducible factor (HIF)-3α in human kidney: suppression of HIF-mediated gene expression by HIF-3alpha. *Biochem. Biophys. Res. Commun.* **287**, 808-813. doi:10.1006/bbrc.2001.5659

Heikkilä, M., Pasanen, A., Kivirikko, K. I. and Myllyharju, J. (2011). Roles of the human hypoxia-inducible factor (HIF)-3alpha variants in the hypoxia response. *Cell. Mol. Life Sci.* **68**, 3885-3901. doi:10.1007/s00018-011-0679-5

Hu, B., Zhang, W., Feng, X., Ji, W., Xie, X. and Xiao, W. (2014). Zebrafish eaf1 suppresses foxo3b expression to modulate transcriptional activity of gata1 and spi1 in primitive hematopoiesis. *Dev. Biol.* **388**, 81-93. doi:10.1016/j.ydbio.2014.01.005

Lee, F. S. and Percy, M. J. (2011). The HIF pathway and erythrocytosis. *Annu. Rev. Pathol.* **6**, 165-192. doi:10.1146/annurev-pathol-011110-130321

Long, Q. M., Meng, A. M., Wang, H., Jessen, J. R., Farrell, M. J. and Lin, S. (1997). GATA-1 expression pattern can be recapitulated in living transgenic zebrafish using GFP reporter gene. *Development* **124**, 4105-4111.

Lorenzo, F. R., Huff, C., Myllymaki, M., Olenchock, B., Swierczek, S., Tashi, T., Gordeuk, V., Wuren, T., Ri-Li, G., McClain, D. A. et al. (2014). A genetic mechanism for Tibetan high-altitude adaptation. *Nat. Genet.* **46**, 951. doi:10.1038/ng.3067

Lyons, S. E., Lawson, N. D., Lei, L., Bennett, P. E., Weinstein, B. M. and Liu, P. P. (2002). A nonsense mutation in zebrafish gata1 causes the bloodless phenotype

in vlad tepes. *Proc. Natl. Acad. Sci. USA* **99**, 5454-5459. doi:10.1073/pnas.082695299

Majmundar, A. J., Wong, W. J. and Simon, M. C. (2010). Hypoxia-inducible factors and the response to hypoxic stress. *Mol. Cell* **40**, 294-309. doi:10.1016/j.molcel.2010.09.022

Makino, Y., Cao, R., Svensson, K., Bertilsson, G., Asman, M., Tanaka, H., Cao, Y., Berkenstam, A. and Poellinger, L. (2001). Inhibitory PAS domain protein is a negative regulator of hypoxia-inducible gene expression. *Nature* **414**, 550-554. doi:10.1038/35107085

Makino, Y., Uenishi, R., Okamoto, K., Isoe, T., Hosono, O., Tanaka, H., Kanopka, A., Poellinger, L., Haneda, M. and Morimoto, C. (2007). Transcriptional up-regulation of inhibitory PAS domain protein gene expression by hypoxia-inducible factor 1 (HIF-1): a negative feedback regulatory circuit in HIF-1-mediated signaling in hypoxic cells. *J. Biol. Chem.* **282**, 14073-14082. doi:10.1074/jbc.M700732200

Maynard, M. A., Qi, H., Chung, J., Lee, E. H., Kondo, Y., Hara, S., Conaway, R. C., Conaway, J. W. and Ohh, M. (2003). Multiple splice variants of the human HIF-3 alpha locus are targets of the von Hippel-Lindau E3 ubiquitin ligase complex. *J. Biol. Chem.* **278**, 11032-11040. doi:10.1074/jbc.M208681200

Maynard, M. A., Evans, A. J., Hosomi, T., Hara, S., Jewett, M. A. and Ohh, M. (2005). Human HIF-3α4 is a dominant-negative regulator of HIF-1 and is down-regulated in renal cell carcinoma. *FASEB J.* **19**, 1396-1406. doi:10.1096/fj.05-3788com

Paik, E. J. and Zon, L. I. (2010). Hematopoietic development in the zebrafish. *Int. J. Dev. Biol.* **54**, 1127-1137. doi:10.1387/ijdb.093042ep

Pasanen, A., Heikkilä, M., Rautavuoma, K., Hirsilä, M., Kivirikko, K. I. and Myllyharju, J. (2010). Hypoxia-inducible factor (HIF)-3α is subject to extensive alternative splicing in human tissues and cancer cells and is regulated by HIF-1 but not HIF-2. *Int. J. Biochem. Cell B* **42**, 1189-1200. doi:10.1016/j.biocel.2010.04.008

Paw, B. H., Davidson, A. J., Zhou, Y., Li, R., Pratt, S. J., Lee, C., Trede, N. S., Brownlie, A., Donovan, A., Liao, E. C. et al. (2003). Cell-specific mitotic defect and dyserythropoiesis associated with erythroid band 3 deficiency. *Nat. Genet.* **34**, 59-64. doi:10.1038/ng1137

Prabhakar, N. R. and Semenza, G. L. (2012). Adaptive and maladaptive cardiorespiratory responses to continuous and intermittent hypoxia mediated by hypoxia-inducible factors 1 and 2. *Physiol. Rev.* **92**, 967-1003. doi:10.1152/physrev.00030.2011

Prabhakar, N. R. and Semenza, G. L. (2015). Oxygen sensing and homeostasis. *Physiology (Bethesda)* **30**, 340-348. doi:10.1152/physiol.00022.2015

Prabhakar, N. R. and Semenza, G. L. (2016). Regulation of carotid body oxygen sensing by hypoxia-inducible factors. *Pflugers Arch.* **468**, 71-75. doi:10.1007/s00424-015-1719-z

Ravenna, L., Salvatori, L. and Russo, M. A. (2016). HIF3alpha: the little we know. *FEBS J.* **283**, 993-1003. doi:10.1111/febs.13572

Semenza, G. L. (2009). Involvement of oxygen-sensing pathways in physiologic and pathologic erythropoiesis. *Blood* **114**, 2015-2019. doi:10.1182/blood-2009-05-189985

Semenza, G. L. (2012). Hypoxia-inducible factors in physiology and medicine. *Cell* **148**, 399-408. doi:10.1016/j.cell.2012.01.021

Semenza, G. L. (2014). Oxygen sensing, hypoxia-inducible factors, and disease pathophysiology. *Annu. Rev. Pathol.* **9**, 47-71. doi:10.1146/annurev-pathol-012513-104720

Shen, C. and Kaelin, W. G.Jr. (2013). The VHL/HIF axis in clear cell renal carcinoma. *Semin. Cancer Biol.* **23**, 18-25. doi:10.1016/j.semcancer.2012.06.001

Sun, K., Liu, H., Song, A., Manalo, J. M., D'Alessandro, A., Hansen, K. C., Kellems, R. E., Eltzschig, H. K., Blackburn, M. R., Roach, R. C. et al. (2017). Erythrocyte purinergic signaling components underlie hypoxia adaptation. *J. Appl. Physiol. (1985)* **123**, 951-956. doi:10.1152/japplphysiol.00155.2017

Yamashita, T., Ohneda, O., Nagano, M., Iemitsu, M., Makino, Y., Tanaka, H., Miyauchi, T., Goto, K., Ohneda, K., Fujii-Kuriyama, Y. et al. (2008). Abnormal heart development and lung remodeling in mice lacking the hypoxia-inducible factor-related basic helix-loop-helix PAS protein NEPAS. *Mol. Cell. Biol.* **28**, 1285-1297. doi:10.1128/MCB.01332-07

Zhang, P., Lu, L., Yao, Q., Li, Y., Zhou, J., Liu, Y. and Duan, C. (2012). Molecular, functional, and gene expression analysis of zebrafish hypoxia-inducible factor-3α. *Am. J. Physiol. Regul. Integr. Comp. Physiol.* **303**, R1165-R1174. doi:10.1152/ajpregu.00340.2012

Zhang, P., Yao, Q., Lu, L., Li, Y., Chen, P. J. and Duan, C. M. (2014). Hypoxia-inducible factor 3 is an oxygen-dependent transcription activator and regulates a distinct transcriptional response to hypoxia. *Cell Reports* **6**, 1110-1121. doi:10.1016/j.celrep.2014.02.011

Zhang, P., Bai, Y., Lu, L., Li, Y. and Duan, C. (2016). An oxygen-insensitive Hif-3alpha isoform inhibits Wnt signaling by destabilizing the nuclear beta-catenin complex. *eLife* **5**, e08996. doi:10.7554/eLife.08996

Zhou, J. G., Feng, X., Ban, B., Liu, J. X., Wang, Z. and Xiao, W. H. (2009). Elongation factor ELL (Eleven-Nineteen Lysine-rich Leukemia) acts as a transcription factor for direct thrombospondin-1 regulation. *J. Biol. Chem.* **284**, 19142-19152. doi:10.1074/jbc.M109.010439

Zhou, X., Guo, X., Chen, M., Xie, C. and Jiang, J. (2018). HIF-3α promotes metastatic phenotypes in pancreatic cancer by transcriptional regulation of the RhoC-ROCK1 signaling pathway. *Mol. Cancer Res.* **16**, 124-134. doi:10.1158/1541-7786.MCR-17-0256

Supplementary Figure S1

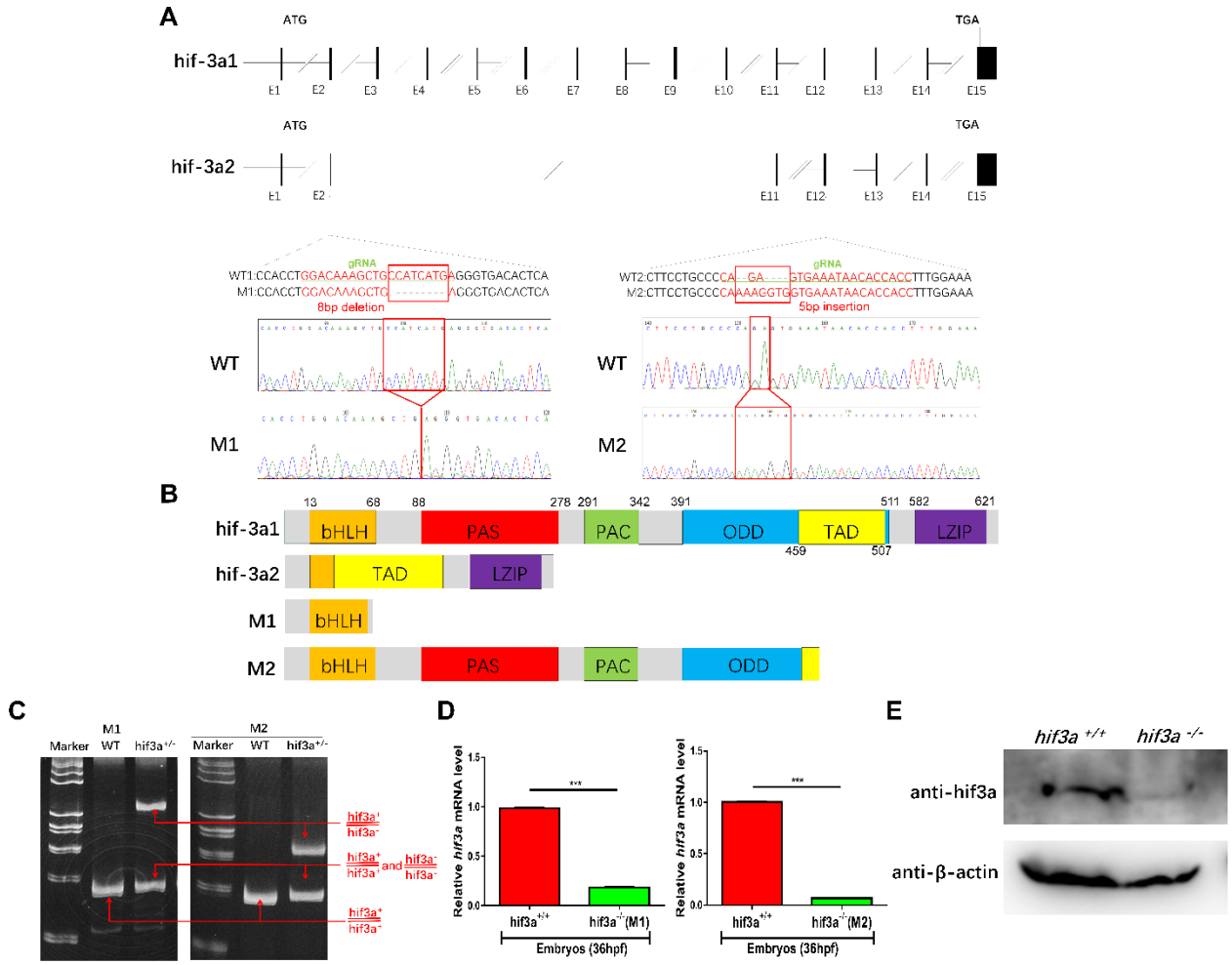

Figure S1. Generation of *hif-3a*$^{-/-}$ zebrafish using CRISPR/Cas9 technology. (A) Schematic of the targeting site in *hif-3a* and the resulting nucleotide sequence in mutant 1 (M1: *Hif-3a*$^{ihb20180620/ihb20180620}$) and mutant 2 (M2: *hif-3a*$^{ihb20180621/ihb20180621}$). (B) The predicted protein products of *hif-3a* in the mutants and their wild-type siblings. (C) Verification of the efficiency of CRISPR/Cas9-mediated disruption of zebrafish *hif-3a* disruption by heteroduplex mobility assay (HMA). (D) The relative mRNA expression levels of *hif-3a* in the wild-type zebrafish and the homozygous mutants (10 embryos for each, 3 replicates; 36 hpf) were quantified by qRT-PCR. (E) *hif-3a* protein level in the wild-type and homozygous mutant embryos (200 embryos) under normoxic conditions detected by anti-hif-3a antibody. *** $p < 0.001$.

Supplementary Figure S2

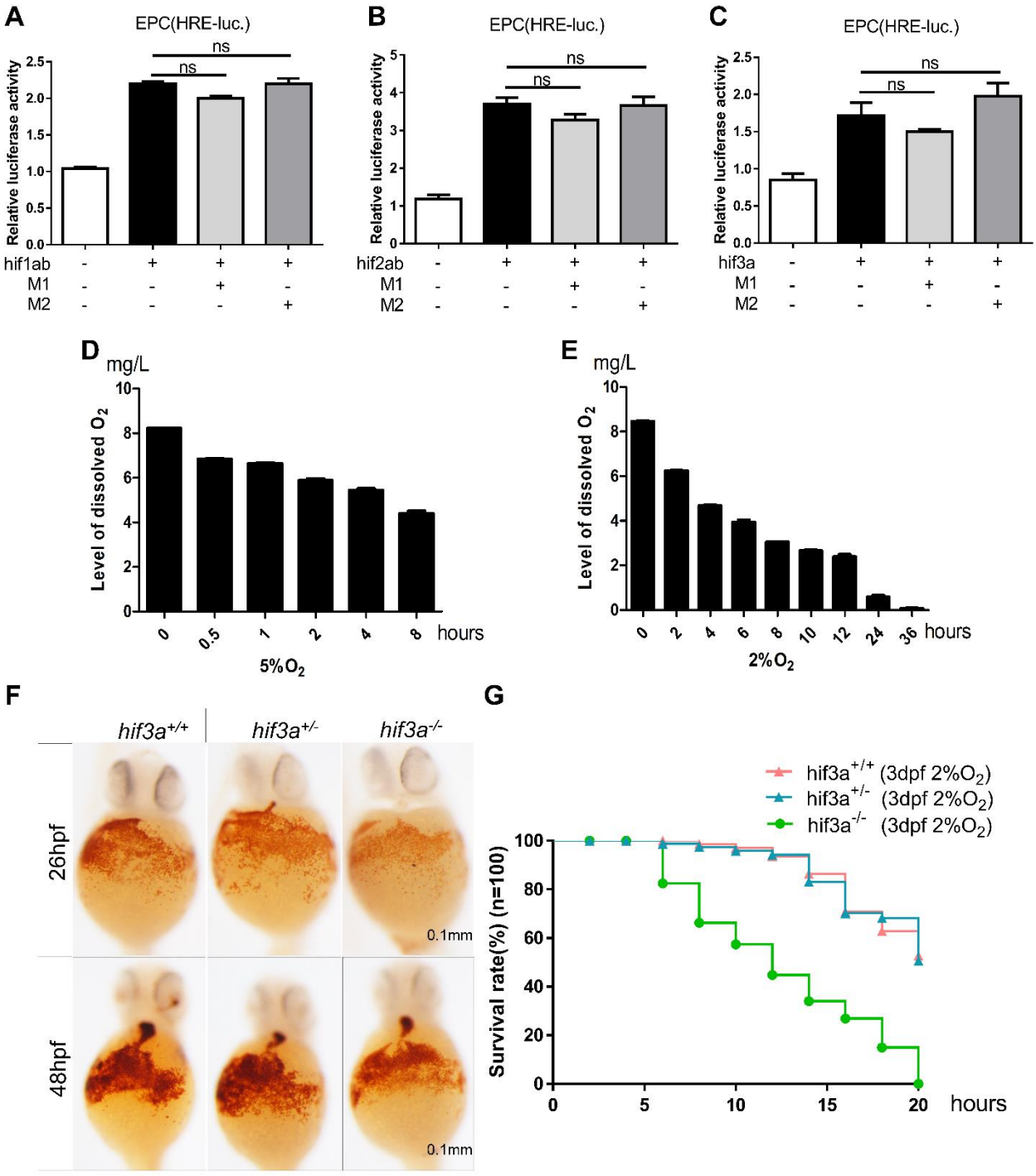

Figure S2. (A, B, C) The predicted truncated proteins in M1 and M2 mutants had no effect on the transcriptional activity of *hif-1ab, hif-2ab* and *hif-3a.* (D, E) The actual levels of dissolved O_2 in water were measured with an LDO101 probe at different time points when the flasks were put into Invivo2 Hypoxia workstation set at 5% O_2 and 2% O_2 respectively (3 replicates). (F) O-dianisidine staining of functional hemoglobin in the mature primitive erythrocytes in *hif-3a*$^{+/+}$ (left), *hif-3a*$^{+/-}$ (middle) and *hif-3a*$^{-/-}$ zebrafish (right) at 26 hpf and 48hpf. (G) The survival rate curve of *hif-3a*$^{-/-}$ zebrafish larvae, *hif-3a*$^{+/-}$ zebrafish larvae and their WT siblings (100 larvae). The oxygen concentration of the hypoxia workstation (Ruskinn INVIVO2 400) was adjusted to 2% prior to experimentation. The dead larvae were counted once every two hours. M1, mutant1; M2, mutant 2; hpf, hours post-fertilization; dpf, days post-fertilization.

Supplementary Figure S3

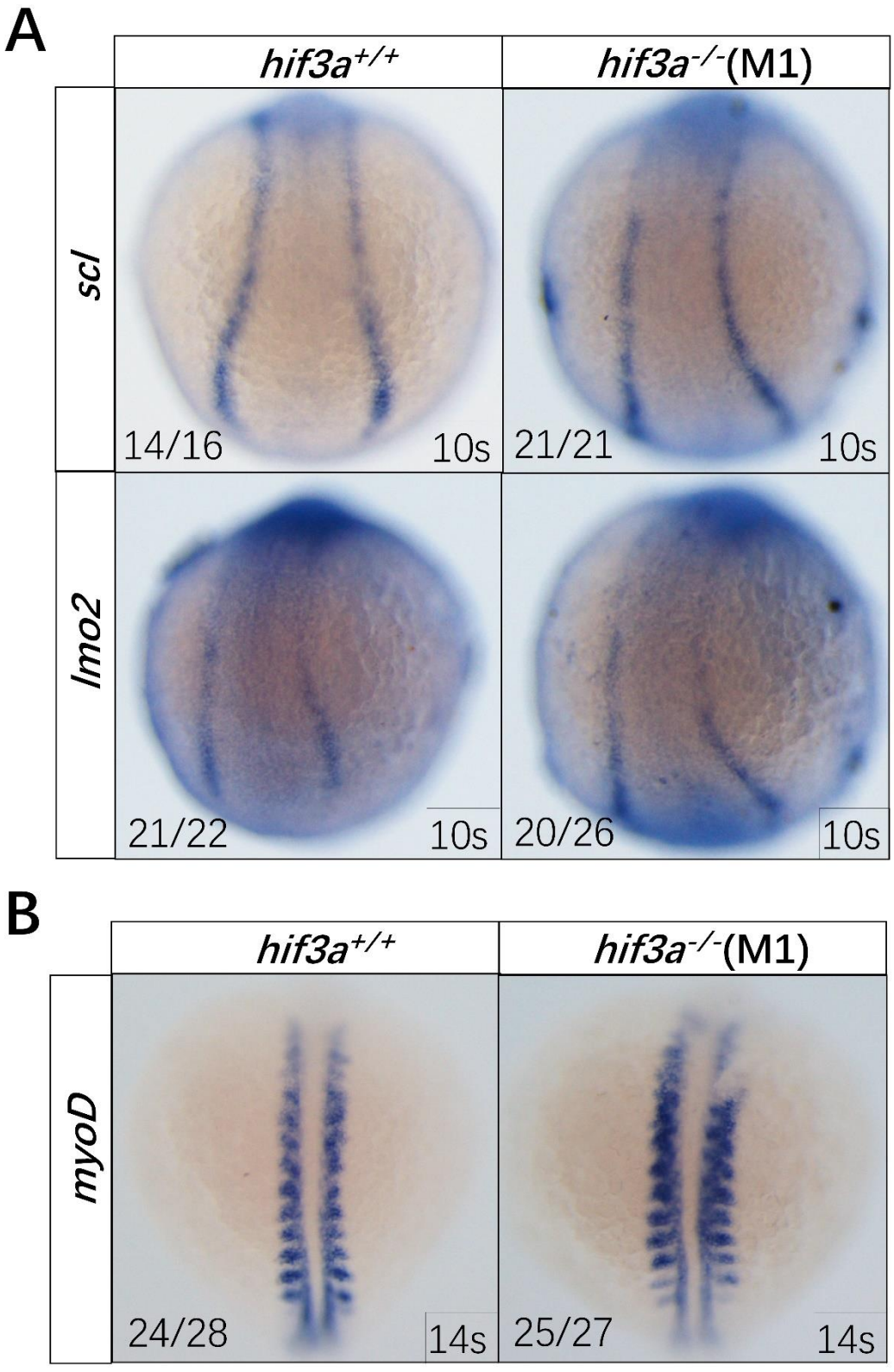

Figure S3. (A) Disruption of *hif-3a* did not alter the expression of *scl* and *lmo2* at the 10 s stage in the posterior lateral mesoderm. (B) Disruption of *hif-3a* did not alter the expression of *myoD* (the somatic mesoderm marker) at 14 s. The number of stained embryos was indicated in the left lower corner of each representative picture. M1, mutant 1; s, somite.

Supplementary Figure S4

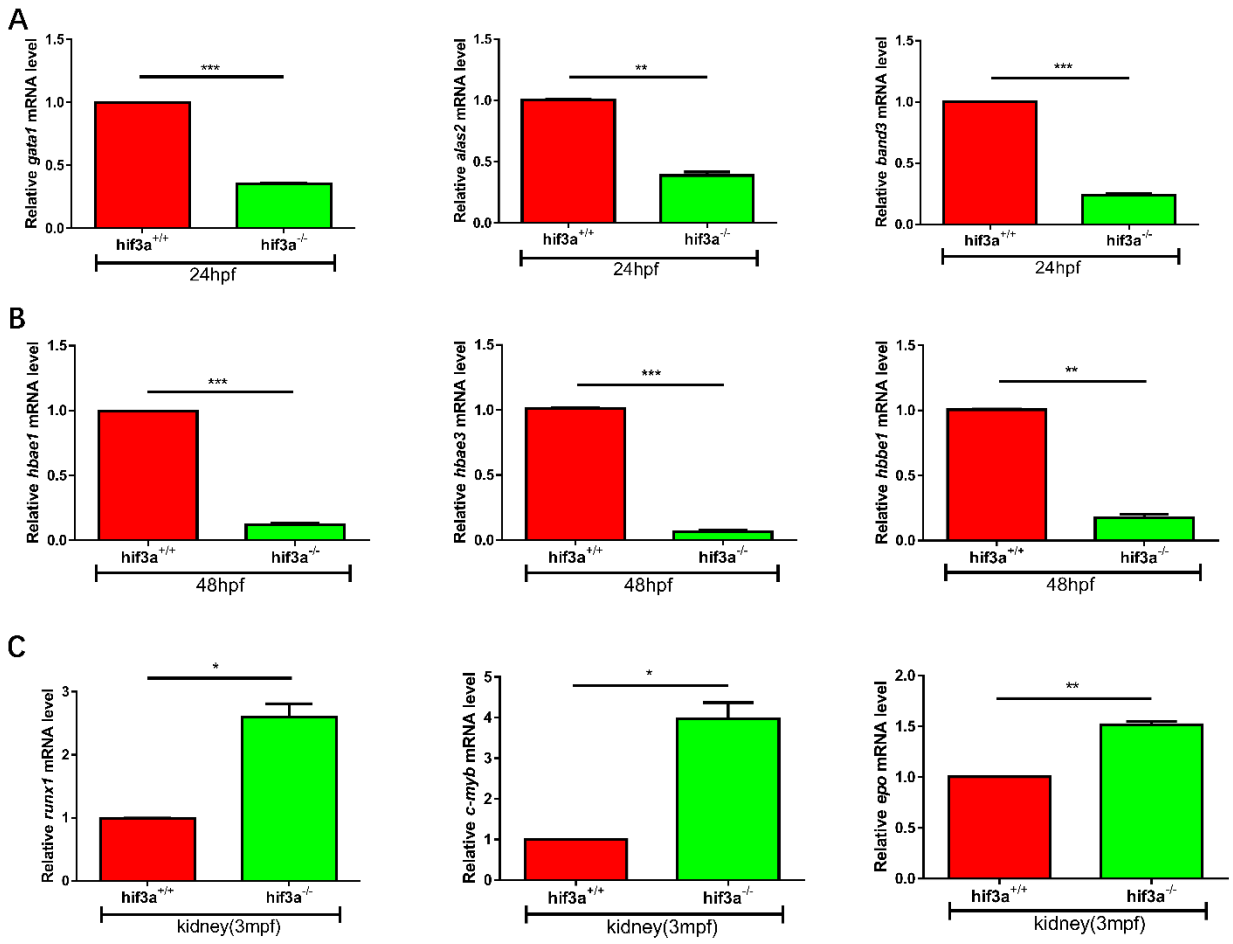

Figure S4. (A) qRT-PCR assays confirmed that the expression levels of *gata1*, *alas2*, and *band3* were reduced in *hif-3a*-null larvae at 24 hpf (30 embryos for each, 3 replicates). (B) Quantitative RT-PCR assays confirmed that the expression levels of *hbae1*, *hbae3* and *hbbe1* were reduced in *hif-3a*-null larvae at 48 hpf (30 embryos for each, 3 replicates). (C) qRT-PCR assays showing that the expression levels of *runx1, c-myb* and *epo* were increased in *hif-3a*-null kidneys at 3 mpf (3 replicates). hpf, hours post-fertilization; mpf, months post-fertilization. * $p < 0.05$; ** $p < 0.01$; *** $p < 0.001$.

Supplementary Figure S5

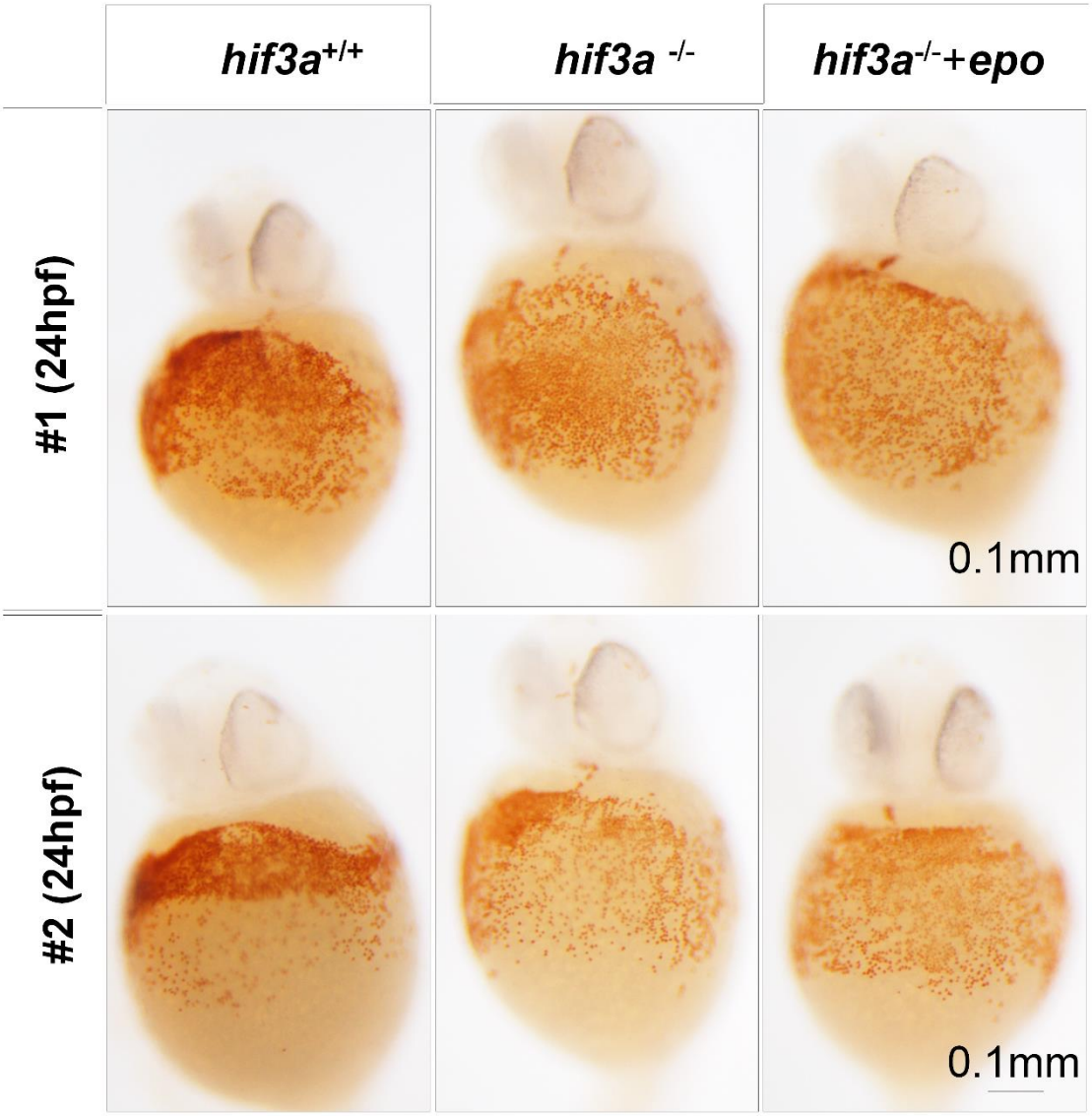

Figure S5. O-dianisidine staining indicated that co-injection of *epo* mRNA (500 pg/embryo) could not restore hemoglobin levels in *hif-3a*$^{-/-}$ larvae at 24 hpf. hpf, hours post-fertilization.

Supplementary Figure S6

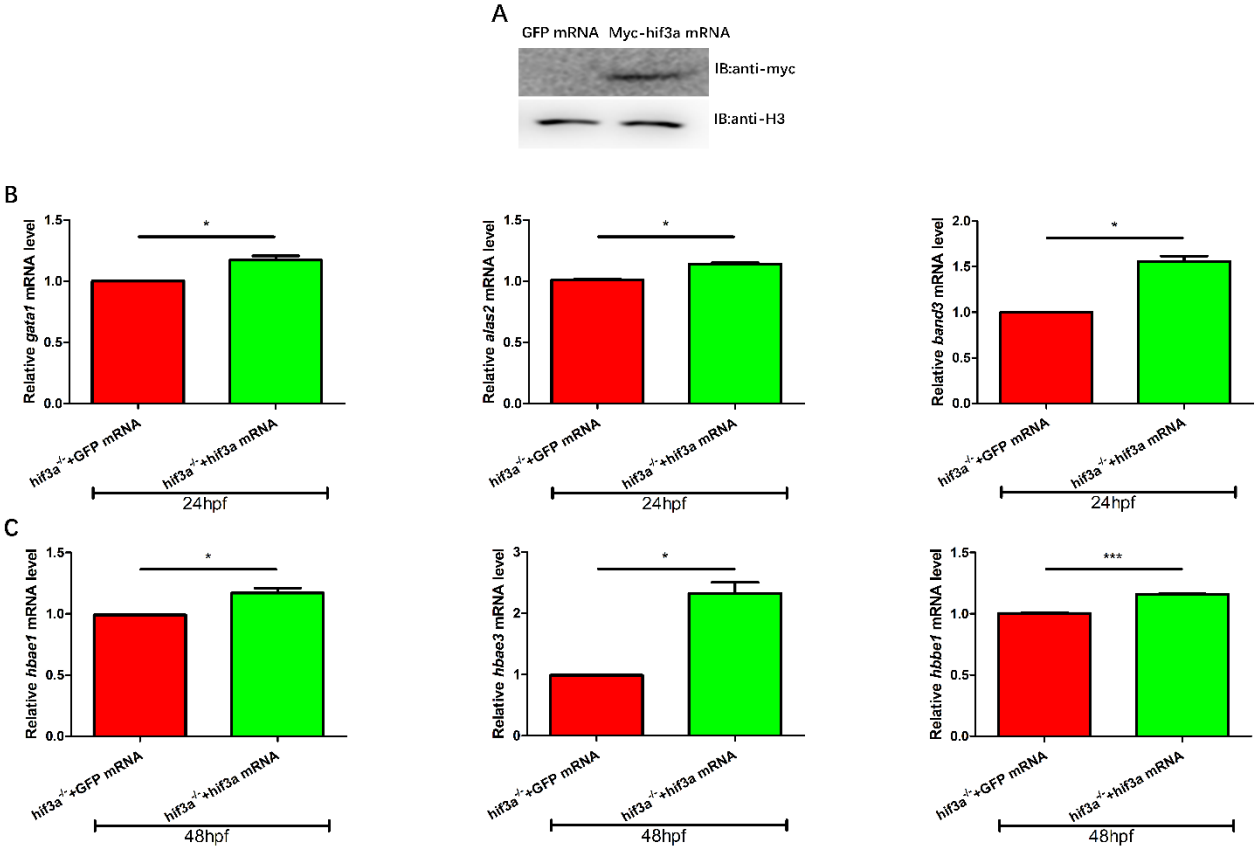

Figure S6. (A) Expression of myc-hif-3a in the injected embryos was confirmed by western blot assays (200 embryos). (B) qRT-PCR confirmed the restoration of *gata1*, *alas2* and *band3* by injection of *hif-3a* mRNA in *hif-3a*-null embryos at 24 hpf as compared with by the injection of the GFP mRNA control. (C) qRT-PCR confirmed the restoration of *hbae1*, *hbea3* and *hbbe1* by the injection of *hif-3a* mRNA in *hif-3a*-null embryos at 48 hpf as compared to the injection of the GFP mRNA control. IB, immunoblotting; hpf, hours post-fertilization. 30 embryos for each, 3 replicates; * $p < 0.05$;*** $p < 0.001$.

Supplementary Figure S7

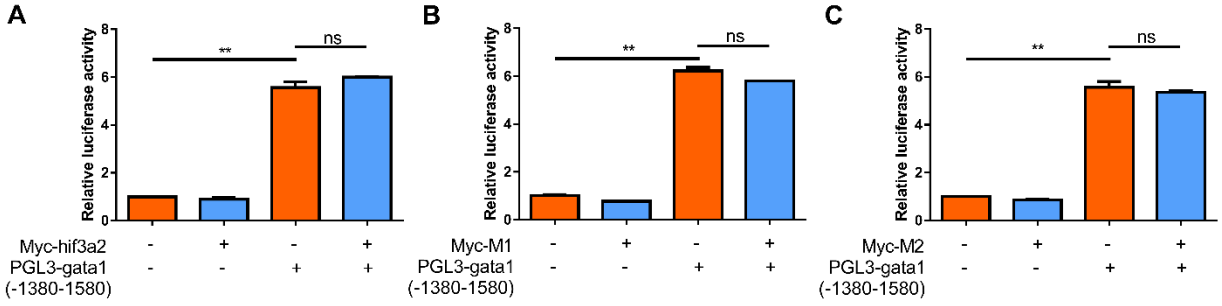

Figure S7. Luciferase reporter assays indicate that *hif-3a2*(A), *hif-3a* mutant M1(B) and M2(C) could not active *gata1* promoter in EPC cells. ** $p < 0.01$; ns, no significance.

Supplementary Figure S8

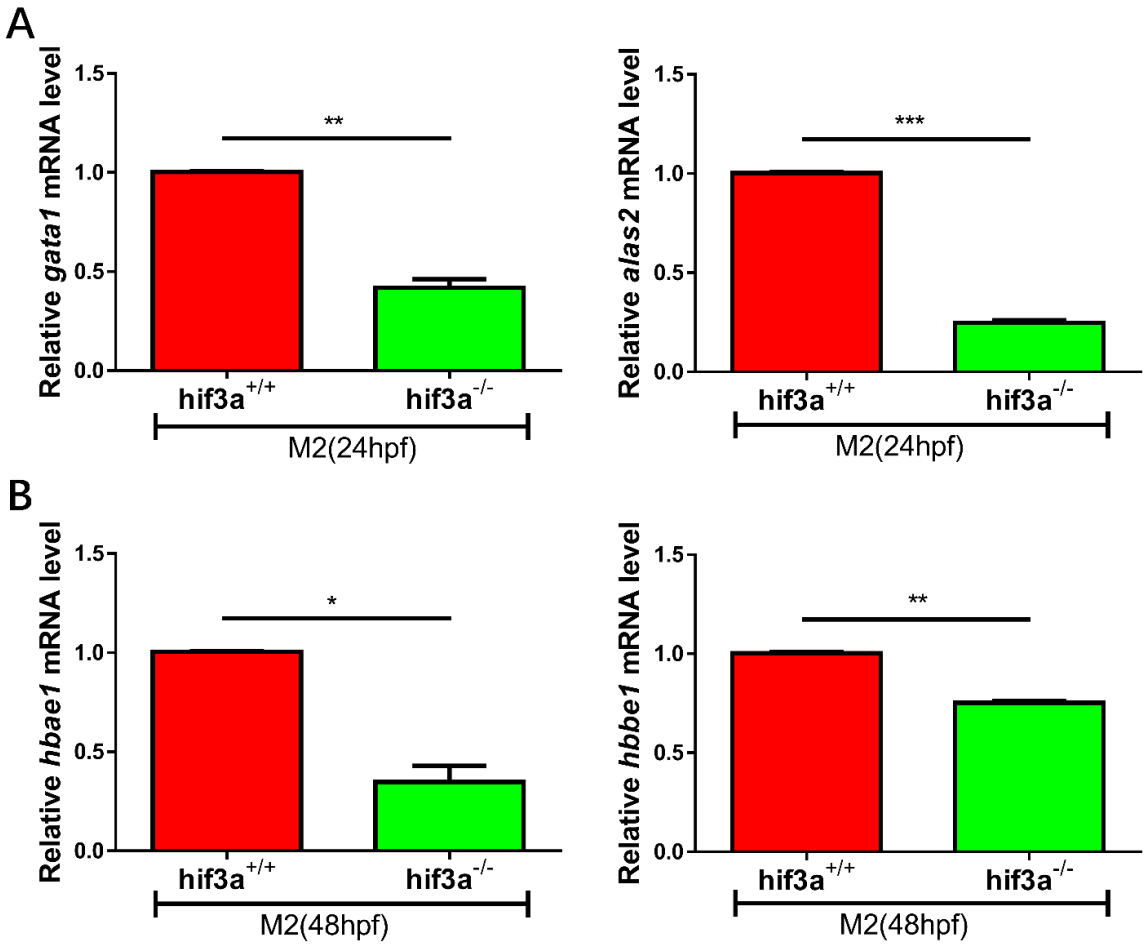

Figure S8. (A) Expression levels of erythrocytic markers *gata1* and *alas2* in wild-type and *hif3a*$^{-/-}$ (M2: *hif1al*$^{ihb20180621/ihb20180621}$) zebrafish larvae at 24 hpf. (B) Expression levels of *hbae1* and *hbbe1* were quantified by qRT-PCR at 48hpf. Values graphed are the means of three independent experiments performed in triplicates; error bars indicate the standard error of the mean (S.E.M.). hpf, hours post-fertilization. n=30; * $p < 0.05$; ** $p < 0.01$; *** $p < 0.001$.

Supplementary Figure S9

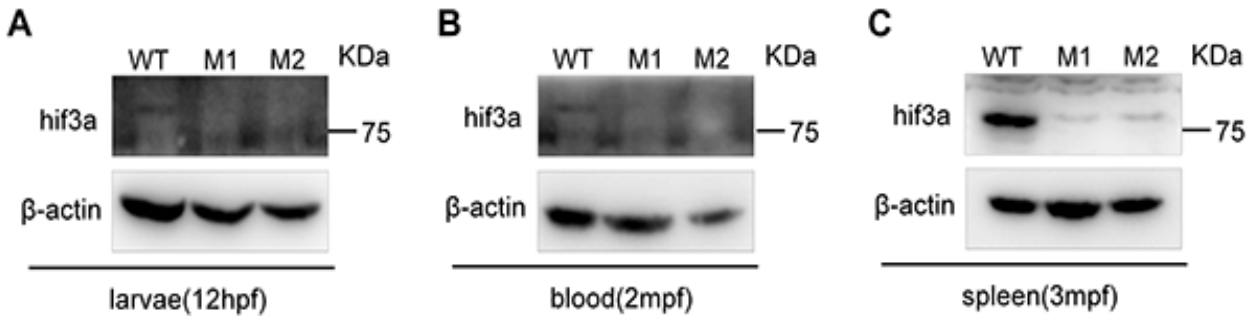

Figure S9. (A, B, C) Western blot analysis of hif-3a protein level in larvae (12hpf; 200 embryos), blood (2mpf; 3 zebrafish for each, 3 replicates) and spleens (3mpf; 3 zebrafish for each; 3 replicates) from wild-type and M1, M2 mutants. WT, wildtype; M1, mutant 1; M2, mutant 2; mpf, months post-fertilization.

Supplementary Figure S10

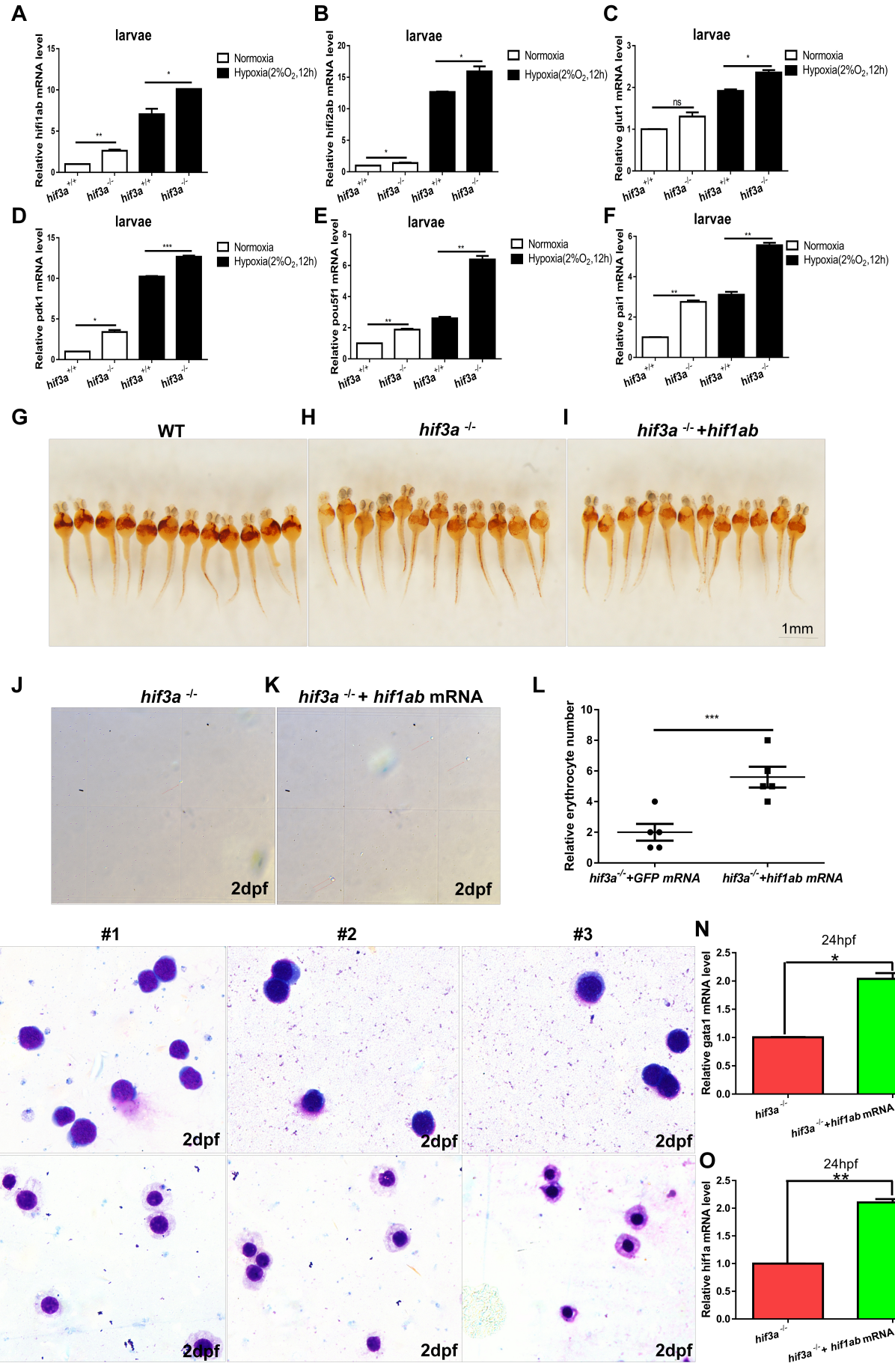

Figure S10. (A, B) qRT-PCR analysis of *hif1a*(A) and *hif2a*(B) expression in WT(*hif-3a*$^{+/+}$) and *hif- 3a*-null(*hif-3a*$^{-/-}$) zebrafish embryo (10 embryos for each, 3 replicates; 3dpf) under normoxia and hypoxia (2% O_2 for 12 hours). (C-F) Expression levels of the *hif-1a* down-stream targets *glut1*(C), *pdk1*(D) and *hif-2a* down-stream targets *pou5f1*(E), *pai1*(F) were increased in *hif-3a*$^{-/-}$ larvae (10 embryos for each, 3 replicates; 3 dpf) under normoxia and hypoxia (2% O_2 for 12 hours). (G-I) O-dianisidine staining indicated that co-injection of *hif-1ab* mRNA (500 pg/embryo) partially restored hemoglobin levels in *hif-3a*$^{-/-}$ larvae at 2 dpf. (J-K) Erythrocyte number counting indicated that co-injection of *hif-1ab* mRNA (500 pg/embryo) increased erythrocyte in *hif-3a*$^{-/-}$ larvae at 2 dpf. (M) May-Grunwald-Giemsa staining indicated that co-injection of *hif-1ab* mRNA (500 pg/embryo) restored erythrocytic maturation in *hif-3a*$^{-/-}$ larvae at 2 dpf. (N) Co-injection of *hif-1ab* mRNA (500 pg/embryo) restored gata1 expression in *hif-3a*$^{-/-}$ embryos at 24 hpf. (O) Expression of micro-injected *hif-1ab* mRNA in *hif-3a* $^{-/-}$ embryos at 24 hpf was confirmed by qRT-PCR. Hpf, hours post fertilization; dpf, days post-fertilization. *$p < 0.05$; ** $p < 0.01$; ***$p < 0.001$.

Supplementary Figure S11

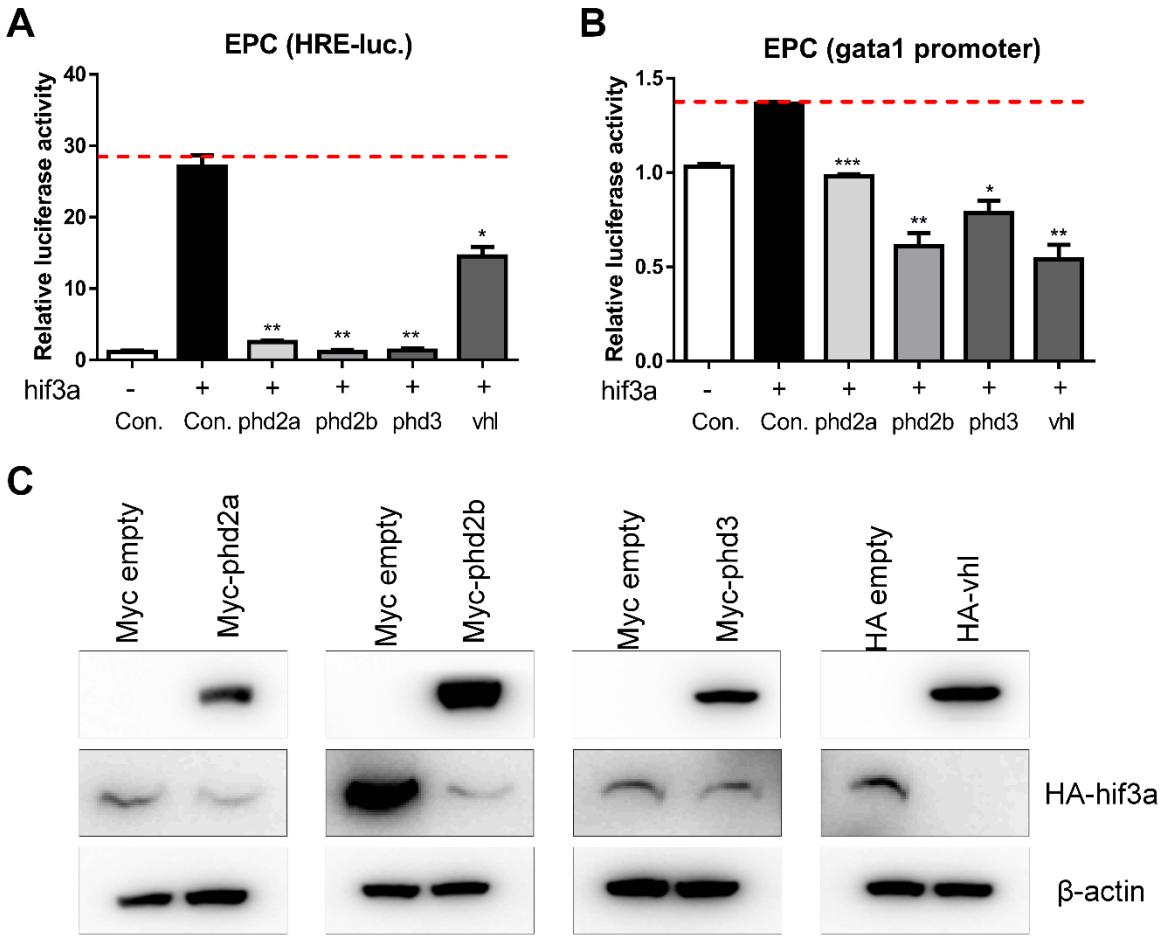

Figure S11. (A) Co-expression of *phd2a, phd2b, phd3* and *vhl* together with *hif-3a* suppressed the activity of HRE luciferase reporter induced by hif-3a in EPC cells. (B) Co-expression of *phd2a, phd2b, phd3* and *vhl* together with *hif-3a* suppressed the activity of gata1 promoter luciferase reporter induced by hif-3a in EPC cells. *$p < 0.05$; ** $p < 0.01$; ***$p < 0.001$. (C) Western blot analysis indicated that hif-3a protein level was decreased when *phd2a, phd2b, phd3* or *vhl* were co-expressed in EPC cells. Con, control. Myc empty, pCMV-Myc empty vector.

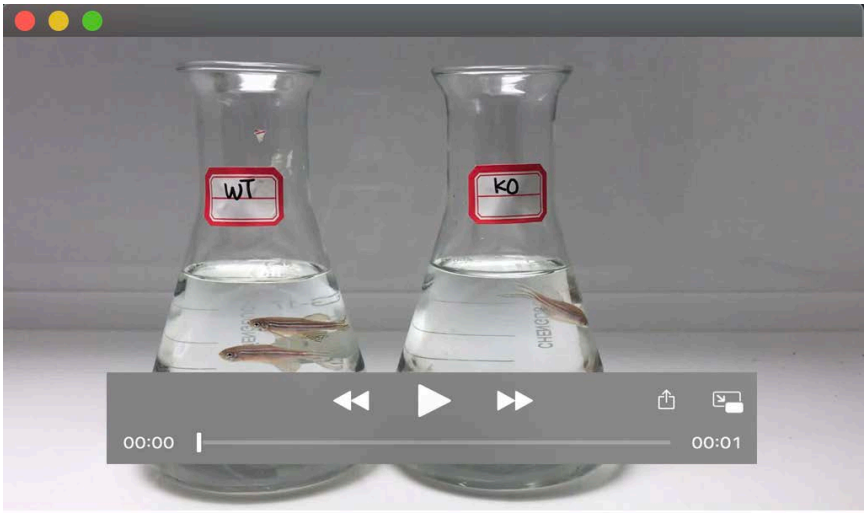

Movie 1. Wildtype (left, WT) and *hif3-a* null (right, KO) zebrafish (3 mpf, body weight = 0.32 ± 0.02 g) placed in a hypoxia workstation at the beginning (5% O_2) (before 30 min).

Movie 2. Wildtype (left, WT) and *hif3-a* null (right, KO) zebrafish (3 mpf, body weight = 0.32 ± 0.02 g) placed in a hypoxia workstation for a while (5% O_2).